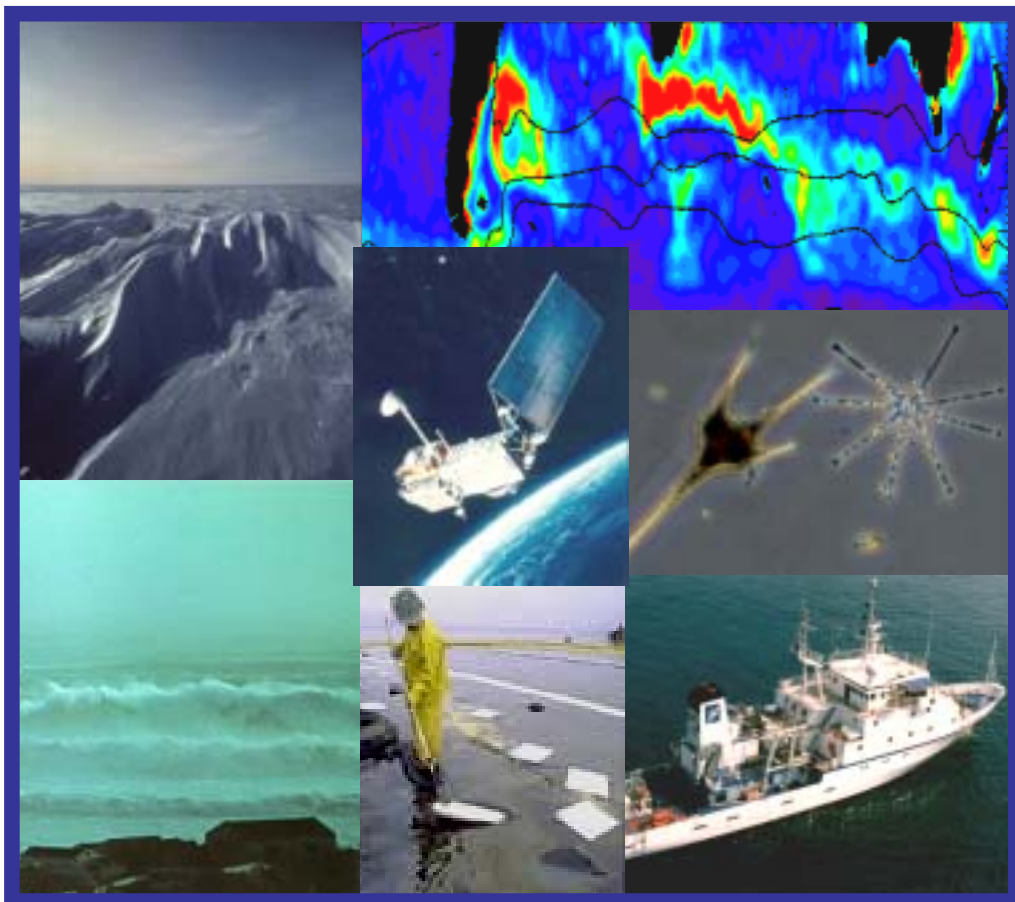


Study of **Innovative Radar Altimeter Systems-IRAC**
in response to ITT AO/1-3912/01/NL/GS
ESA contract n. 15737/01

Report by the IRAC science team



coordinated by:

ISAC Istituto di Scienze dell'Atmosfera e del Clima

(CNR-Consiglio Nazionale delle Ricerche)

Satellite Oceanography Group

Rosalia Santoleri

Bruno Buongiorno Nardelli

participants:

ENEA-Ente Nazionale per l'Energia e l'Ambiente

Global Mediterranean Climate Section

Massimo Frezzotti

Salvatore Marullo

INGV-Istituto Nazionale di Geofisica e Vulcanologia/Università di Bologna

Nadia Pinardi

ISGDM-Istituto per lo Studio della Dinamica delle Grandi Masse

(CNR-Consiglio Nazionale delle Ricerche)

Luigi Cavaleri

SOC-Southampton Oceanography Centre

Laboratory for Satellite Oceanography

Peter Challenor

Paolo Cipollini

Christine Gommenginger

Table of contents:

1. Introduction.....	3
2. Large scale phenomena and related requirements.....	6
3. Open ocean mesoscale and marginal seas circulation.....	11
4. Measuring small scales: sub-mesoscale structures and coastal processes.....	21
5. Operational oceanography.....	27
6. Ocean surface winds and waves.....	32
7. Ice sheet dynamics.....	40
8. References.....	43
9. Appendix.....	48

1.Introduction

In the last decades, satellite remote sensing demonstrated to be a powerful tool to study the ocean and ice surface on a global scale. As an example, during WOCE (World Ocean Circulation Experiment) the only true global observations made with regular sampling in space and time were obtained by space-borne sensors. However, the opacity of the ocean to electromagnetic signals has limited most measurements to the very top surface layer of the ocean (sea surface temperature and colour), or to the ocean-atmosphere interface (winds and waves). On the other hand, the measure of radar altimeter range gave the opportunity to obtain information also on the dynamics of the ocean at greater depths. Range determination from space also allowed to obtain the most accurate near-global coverage of ice sheet surface elevation to date and provided important estimates on the inter-annual and long-term changes of ice volume and polar precipitation redistribution that may be associated with climate change

Variations in sea surface height are associated both to dynamical and thermodynamical processes. Actually, the sea elevation is related to the heat content of the whole water column, as the volume of water is modified mainly by temperature, and to a minor extent by salt variations. Moreover, the ocean responds to the gravitational attraction of the sun and moon, rising and falling each day with amplitudes that can reach several meters. Tides are an important mechanism that has a strong impact in oceanography, and whose study took great advantage from altimetry.

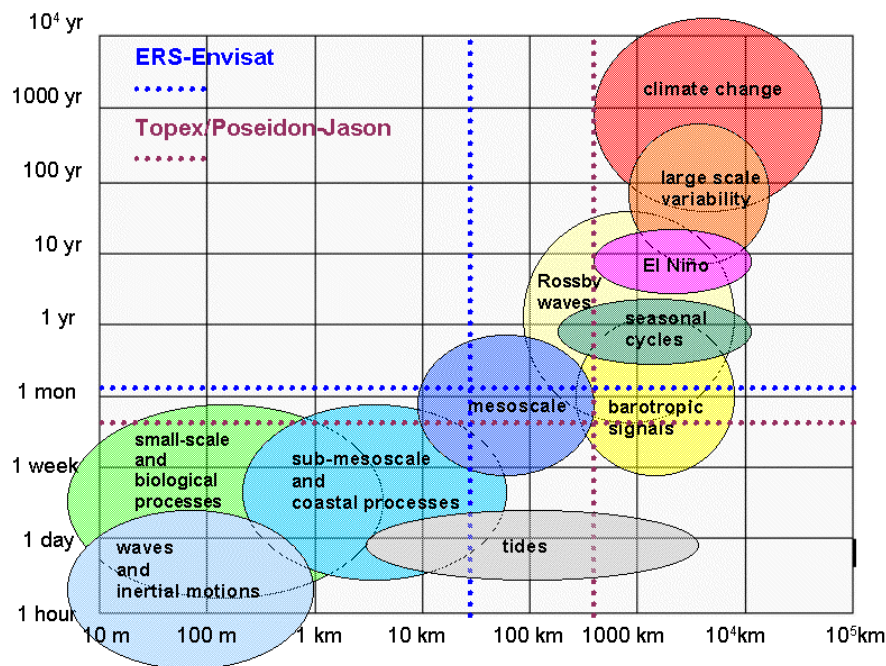


Figure 1.1. Schematic view of the approximated space-time scales of major processes occurring in the ocean. Superimposed lines represent Envisat and Jason sampling characteristics.

The ocean surface dynamics is thus the result of many processes. These are characterized by different space and time scales, that range in time from hours to

thousands of years, and from meters to hundreds of kilometers in space. In figure 1.1, a diagram of the space-time scales of major processes occurring in the ocean is presented. It is evident that there are many processes that occur on the temporal and spatial scales that are not resolved by present satellite observations. Up to now the repeat cycles of T/P and ERS missions permit to measure large scale SSH fields for studies of ocean variability on monthly and longer time scales and space scales of few hundred of kilometres. No information is available on processes at shorter space and time scales such as coastal processes, large scale barotropic signals, but also to extract information of mesoscale dynamics is problematic. However, a large fraction of the eddy kinetic energy of the ocean is concentrated in eddies and currents with spatial scales shorter than resolved by the sampling of present altimeters. Consequently, a new challenge of the future altimeter mission should be to obtain high resolution measurements.

In spite of the potential value of altimeter data, a limit is still given by accuracy, which, for oceanic applications, as an example, should be increased to ~ 1 cm (Wunsh and Stammer, 1998; Chelton et al. 2000). Also other factors influence the effective use of altimeter data.

Presently available geoid models have errors smaller than oceanographic signals only at wavelengths longer than 3000 km, while for oceanic applications an accurate measure of the geoid is obviously needed to obtain absolute surface geostrophic currents from altimeter range, while. As a consequence, altimeter-derived absolute ocean topography could be used to test general circulation models only at the larger scales. Without detailed knowledge of the geoid, satellite altimeter data have been used to study the variability of ocean surface topography, limiting the potential use of the altimeter data. Substantial improvements are expected in the future thanks to the GRACE and GOCE geodetic mission. With a better estimate of the geoid, it will be possible to compute the absolute geostrophic currents, improving significantly the knowledge of ocean general circulation and the assimilation of altimeter data in numerical models.

Probably, the most important limitation for any application is represented by the space and time sampling of present altimeters. In fact, measurements of ocean and ice topography, winds and waves by radar altimeters inevitably involve a trade-off between spatial and temporal resolution. Improvement of spatial resolution implies a degradation of time sampling with obvious consequence to the data usefulness. A clear example of the above limitation is given by the ERS-1 Geodetic phase during which the distance between tracks was reduced to 0.12° of longitude, but the revisit time of 168 days made such data not useful for oceanographic applications. This trade-off between spatial and temporal resolution guided the compromise in designing altimeter missions. The 10-days repeat cycles of T/P-Jason corresponds to 316 km spacing of ground tracks at equator. The 35-days repeat of ERS-ENVISAT corresponds to 39 km spacing of ground tracks at equator. This time and space sampling limits the scales of phenomena that can be resolved by these altimeters.

Major requirements for the application of altimeter data have already been identified and need to be emphasized, being of fundamental importance to the design of future missions. On one hand, the continuity of the data records is crucial for studies on climate change effects on sea level rise. On the other hand, the sampling density is still very poor, even after combination/merging of different satellite data. High resolution mapping is the

most important improvement required by studies of the mesoscale, which is the most energetic scale in the oceans, and on coastal processes, where the largest economical and social interests are concentrated, and is also needed by operational models to achieve more precise forecasts. The main objective of this report is then to describe the limits and capabilities of present altimeters in monitoring the ocean and ice topography as well as wind and waves, and to provide more precise indications on the scientific requirements for future altimeter systems. However, providing a complete review of the oceanographic and ice applications of altimeter data is obviously beyond the scope of this report. Consequently, only some key examples of the use of altimeter data will be presented, posing the most stringent requirements on accuracy, spatial and temporal sampling and length of the time series. However, the identified requirements can be assumed as 'optimal', as they actually cover the main processes occurring on a wide range of spatial and temporal scales.

2. Large scale phenomena and related requirements

Large scale dynamics in the ocean covers a range of different phenomena, whose spatial extent is significantly greater than the Rossby radius of deformation (which is typically a few tens of kilometres at mid-latitude). Rather than examining here all the different classes of phenomena, in what follows we identify and discuss three broad classes posing the most stringent requirements on spatial sampling, length of the time series and temporal sampling, respectively. The identified requirements can be assumed as 'optimal' requirements for the monitoring of all large-scale phenomena.

2.1 Planetary waves

Extra-equatorial planetary waves (also known as Rossby waves) are long-wavelength (100s-1000s km) internal waves whose existence is due to the shape and rotation of the earth and to the conservation of potential vorticity. These waves travel from east to west across all the ocean basins, at a speed increasing equatorward, from 1-2 cm/s at latitudes of 40° to a few tens of cm/s at about 10° latitude (in the equatorial band, roughly between $5S$ and $5N$, planetary waves are governed by different dynamics and we do not cover those here). Figure 2.1, from Cipollini et al. (2000) shows the schematic of a first-mode baroclinic planetary wave. Despite the main disturbance being in the thermocline, with an amplitude of 10-100 meters, those waves can be seen by an altimeter in virtue of the small (a few cm) signature at the surface.

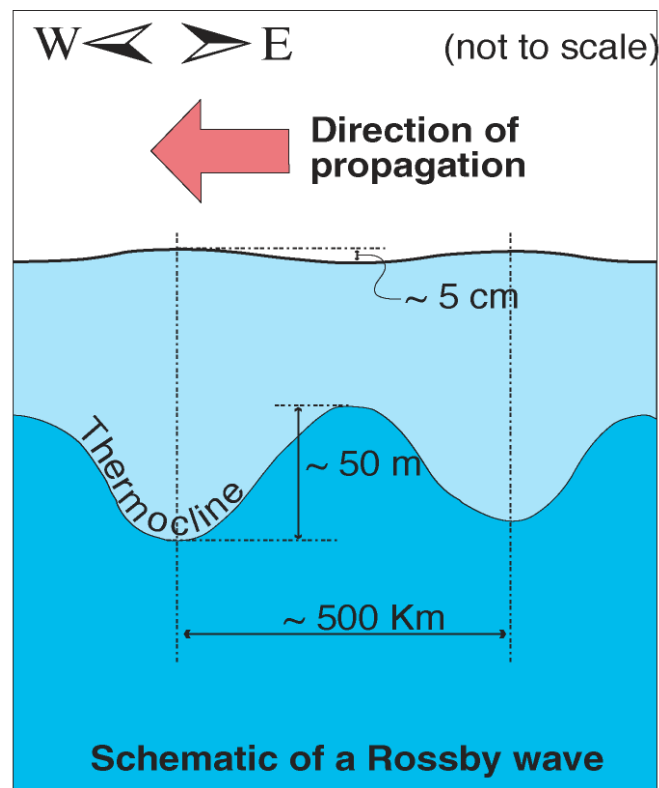


Figure 2.1 - Schematic of a first-mode baroclinic Rossby wave

Planetary waves play a key role in setting the large-scale ocean circulation, by maintaining the western boundary currents. As they slowly transmit to the western part of the ocean information about events (forcing) happened in the eastern part, they can delay the effects of major climatic anomalies like El-Niño. Jacobs et al. (1994) present evidence for the existence of an extra-tropical Rossby wave in the North Pacific, generated by the El Niño event of 1982-83, and suggest that after a decade's delay this wave induced a shifting of the Kuroshio Current in the north-west Pacific which may have affected the climate of North America, and which may have been responsible for the dramatic meteorological events in North America in 1993, such as the Mississippi flooding (McPhaden, 1994). In short, as well as being one of the ways the ocean itself responds to climate events, Rossby waves may also delay the effects of these events and control the dynamics of climate change and weather variability.

The above is just one possible example to illustrate the keen interest in planetary waves by oceanographers and climatologists. Another one would be that the proper rendition of planetary wave is a good testbed for the realism of ocean models. Speed of Rossby waves is an important parameter, as it sets the response time of the oceans to a vast range of events. The advent of satellite altimetry has allowed the observation of these waves in the global ocean (Chelton and Schlax, 1996) and they have been found to travel up to twice or three times faster than the standard theory predicted. This apparent discrepancy has prompted a number of theoretical studies to reconcile theory and observations, culminated in the various theory extensions by Killworth and collaborators (Killworth et al. 1997, Killworth and Blundell, 1999).

Recently, the signature of Rossby waves has been observed globally also in SST (Hill et al., 2000) and ocean colour (phytoplankton chlorophyll) data (Cipollini et al, 2001, see fig. 2.2; Uz et al, 2001). The problem has then arisen to explain the nature of this signature in the non-altimetric datasets. Is it simply due to horizontal north-south advection of phytoplankton and SST gradients, in turn due to the geostrophic velocities associated with the propagating waves? Or are there vertical mechanisms in place, such as upwelling of nutrients as a result of the isopycnal displacement due to the passage of the waves, at least in some locations? The latter hypothesis holds a particular interest to biologists and has potential repercussions on the global carbon cycle. Siegel (2001) has hypothesized that planetary waves could, by lifting the isopycnals on their passage (the so-called 'rototiller effect'), contribute to maintain a background productivity in the most oligotrophic areas of the ocean in non-bloom condition, thus keeping the phytoplankton population ready to bloom when the right conditions appear. The investigation on what mechanism predominates must necessarily examine the phase relationship between the wave signatures in the different datasets, as, for instance, the phase differences between SSH and ocean colour due to advection and upwelling are different. A study carried out at the Southampton Oceanography Centre (manuscript in preparation), by modelling the various mechanisms and comparing the modelled phase relationship with that from the SSH/ocean colour observations, has showed that advection of phytoplankton gradients is the predominant mechanism over large regions of the oceans, but a significant contribution by vertical processes cannot be ruled out yet, at least in some regions, and further research is necessary.

Rossby waves observed in global ocean colour data at SOC Example: Indian Ocean, 35.75°S

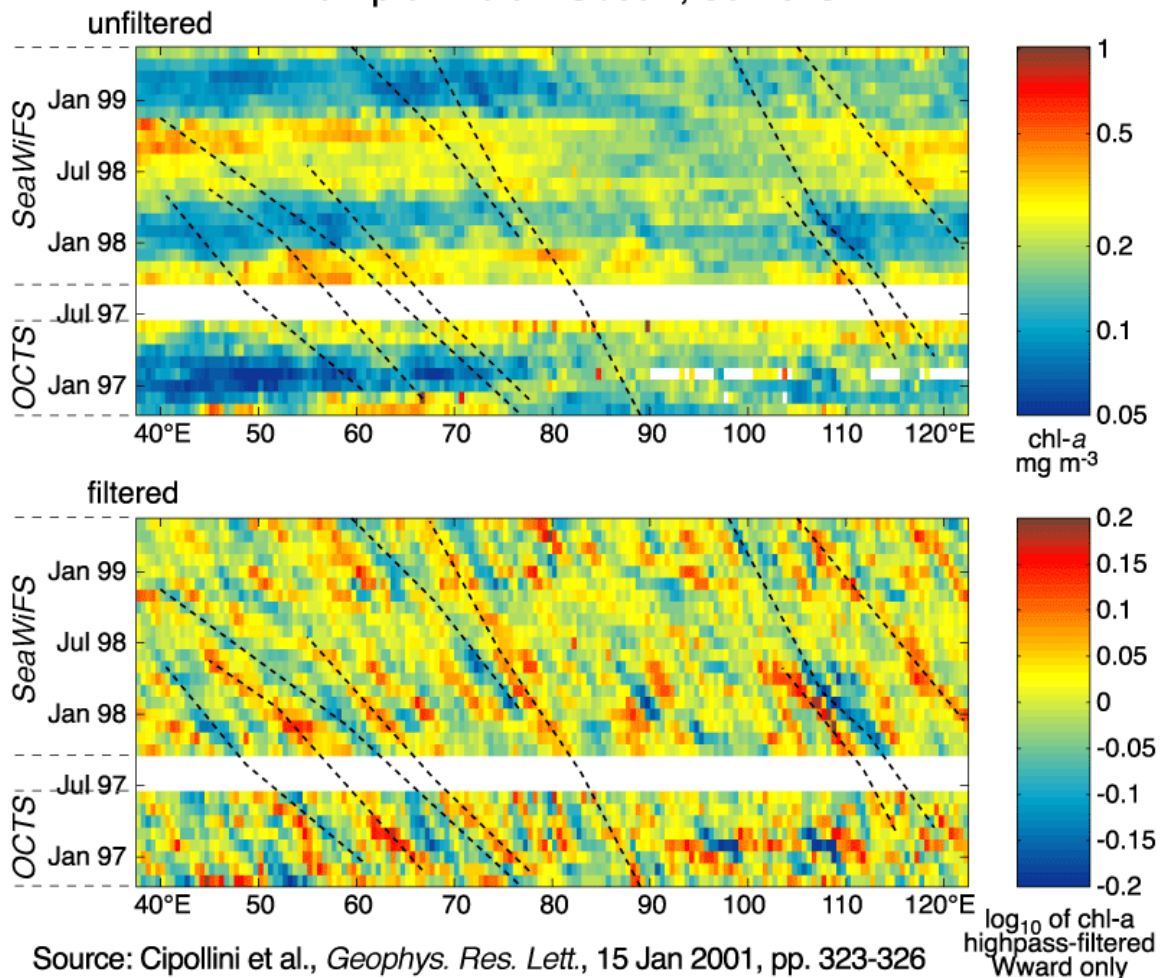


Figure 2.2 – Example of observation of planetary waves in fields of ocean colour data (phytoplankton chlorophyll concentration)

2.2 Altimeter requirements for the observation of planetary waves

Over the latitude range where extra-equatorial planetary waves propagate (5-10 to 40-50 degrees) both their speed and their wavelength vary by almost two orders of magnitude (50 to 1 cm/s, and 10000 to 300 km, respectively). While at low- to mid-latitudes (5-35 degrees) the space-time sampling characteristics of both T/P / JASON and ERS / Envisat are well suited for their observation (at low latitudes, a time resolution of ~days can still be obtained, in virtue of the much lower space resolution needed), T/P has problems at higher latitudes due to the spacing of the tracks which is comparable with the horizontal scale of the phenomenon, so that the signature of the waves can ‘disappear’ between two adjacent tracks. The accuracy required is of the order of 2cm for the smaller signals, especially at high latitude where the wave amplitude is much reduced – but in many parts of the oceans the amplitude is of the order of 10 cm.

Those requirements become much more stringent for the study of the bio-physical interactions due to the waves. The SSH signal has to be compared to SST and ocean colour signals which are commonly available at high space/time resolution (normally we use 0.5 degrees by ten days). The analysis of the phase relationship between the different signals (and in particular the need for resolving phase shift of a few tens of a radians, which might enable us to assess the relative contributions of horizontal and vertical mechanisms) would thus require comparable SSH fields, say at ~50 Km resolution every ten days, at ~1 cm accuracy.

Another important issue is to avoid tidal aliasing, or to confine it to spectral regions of limited relevance for oceanography. For instance, the Geosat sampling pattern aliased the M2 tide to frequencies and wavelengths which cannot be discerned from those typical of mid-latitude planetary waves, thus making the early detection of planetary waves difficult. T/P and JASON are largely free of this problem, although a residual K1 component can be present. ERS/Envisat may have more problems due to the sun-synchronous orbits. The need for avoiding tidal aliasing, and thus for appropriate orbit configuration design and for very accurate tidal models to be employed in the processing scheme, is paramount.

2.3 Very large-scale propagating anomalies in the North Atlantic

Sutton and Allen (1997) have shown that very large-scale (thousands of km) SST anomalies propagate eastward in the North Atlantic off Cape Hatteras and towards the European continent. This is believed to have significant effects on European climate and its interannual variability and could be the key to the development of prediction tools.

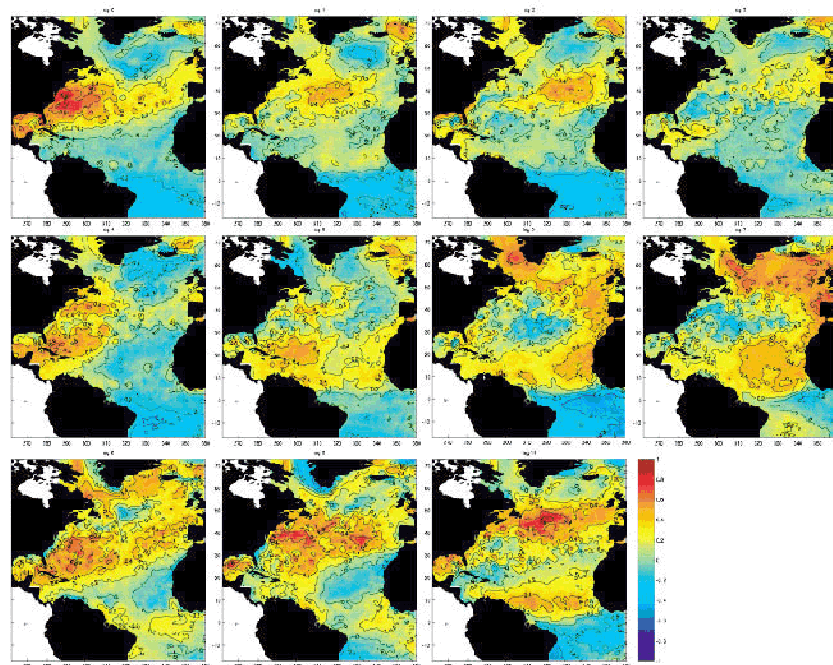


Figure 2.3: multi-year lag correlations (0 to 10 years, left to right and top to bottom) of North Atlantic SST with respect to the temperature in the Cape Hatteras region.

Recently, Houseago-Stokes and Challenor (2002) found a clear four-year signal in the SST anomalies (see Figure 2.3 which shows multi-year lag correlations of North Atlantic SST with respect to the temperature in the Cape Hatteras region). For a better characterization of these signals and of their effects on the density field, they need to be studied in the altimetric signal too. This obviously poses a requirement on the length of the time series (~decades) and also indicates that the intercalibration of successive missions should always remain a high priority.

2.4 Fast barotropic signals

Fast, high frequency barotropic signals with periods of just a few days or less are the oceanic response to fast transient atmospheric forcing fields. According to Stammer et al. (2000) a significant part of the extra-tropical energy in the oceans lies in the period band of 3-10 days, especially at high latitudes. These high frequency signals, which also include barotropic planetary waves (Gaspar and Wunsch, 1989) are obviously aliased by the spacecraft sampling and might account for most of the residual 'trackiness' on SSH maps. Thus they need to be removed. There are two possible approaches

- to model the signal and remove it
- to try and observe it

But even the first one (i.e. modelling) calls for a better knowledge of these phenomena, so that an observational approach seems appropriate in any case. This raises very stringent requirements on time sampling, at least 3 days over 500 km and ideally 1 day over 300 km, at ~1 cm accuracy.

2.5 Summary of requirements

The need for observing the different classes of phenomena described above leads to different sampling requirements. The study of planetary waves would essentially benefit from better space sampling. The observation of very large-scale anomalies requires long time series of altimeter data and an accurate intercalibration of subsequent missions. Finally, a better knowledge of how barotropic energy propagates, which is important not only in itself but also to improve the quality of the corrected altimeter data, can only be achieved with better sampling in time. The need for increased sampling both in space and time might suggest constellations of altimeters, but it is interesting to note that also some of the new altimeters concepts considered in this project seem capable to provide the needed coverage.

Two final considerations to be kept in mind when designing future missions are the following:

- the geoid issue. The geoid is not known with sufficient accuracy at present, so all nadir-looking systems have to use repeat track orbits, but with the GRACE mission just launched and GOCE coming soon, this need may disappear in few years, resulting in much more freedom in choosing the orbit pattern.
- the tide issue. Avoiding tidal aliasing (or confining it to spectral regions of limited relevance to oceanography) remains paramount for observations of propagating signals in the oceans.

3. Open ocean mesoscale and marginal seas circulation

The open ocean surface as observed from space imagery mainly shows whirling structures, meanders and fronts that change with time. It can be roughly stated that the spatial and time scales of most of the ocean variable features range between a few tens and a few hundreds of kilometers (~ 50 or even less $\div \sim 500$ km) and between ~ 10 and ~ 100 days. These scales actually correspond to what is known in literature as open ocean mesoscale, and but also to the quasi-permanent circulation features (such as small gyres) found in marginal seas. Even if there is not a precise definition of the spatial and time scales of the mesoscale, its lower limit is defined by the baroclinic *Rossby radius of deformation* (Gill, 1983), that can vary from place to place, ranging from ~ 40 km (if calculated using numbers characteristics of the Gulf stream off Cape Hatteras, for example) to ~ 10 km (if estimated in the Mediterranean Sea).

The mesoscale variability is the dominant signal in the ocean circulation. In particular, the western boundary currents, but also the Antarctic Circumpolar Current (ACC), are areas of intense mesoscale variability. However, mesoscale signals are observed everywhere in the global ocean surface, mainly along frontal zones. Here, the higher level of eddy kinetic energy is primarily related to instabilities of the mean flow due to both baroclinic and barotropic instabilities. In the first case (under baroclinic instability conditions), the presence of a vertical shear in the mean flow produces a release of available potential energy to eddy potential and kinetic energy while in the second case (barotropic instability) a significant horizontal shear leads the mean flow to release kinetic energy to the eddy field (Eddy Kinetic Energy). Far from region of strong currents, where a weaker mesoscale activity is observed, the variability can be driven by wind fluctuations (small scale wind stress curl variations), interaction of the current with the bottom topography or other topographic obstacles such as islands.

Both mesoscale and sub-basin structures play a fundamental role in the global ocean circulation, climate and have a significant impact on the marine ecosystem functioning. In fact, mesoscale eddies can transport mass and properties such as heat, salt and chemical tracers. Moreover, the ocean primary production (fixation of atmospheric CO_2 into organic matter) is modulated through the large vertical motions and changes in the depth of the mixed layer associated to both mesoscale eddies generation and to the interaction between atmosphere and the ocean surface in the quasi-permanent vortices found in semi marginal seas.

All of these considerations underline the crucial importance of the mesoscale phenomena in the ocean and suggest the necessity of better understand the basic processes also requiring a more complete and extensive global observing system. Altimeter data can substantially contribute to this goal.

Altimeter data have already provided important quantitative results in the monitoring and study of the ocean mesoscale. From November 1986 to June 1989 Geosat provided the first long duration (3 years on a near-repeat orbit of 17.05 day cycle) altimeter mission with enough low noise level suitable for mesoscale observations. Successively, in 1991 ERS-1 started to operate (35 days repeat cycle) and Topex/Poseidon (10 days repeat cycle) was operating since 1992. From December 2001 also JASON-1 is operating on the same orbit of Topex/Poseidon approximately one minute (approximately 370 km) ahead on an identical ground track. The analysis of these data permitted to improve the

knowledge of the ocean mesoscale but also contributed, on the basis of the scientific results, to the understanding of the limitations of the present altimeter observation systems.

Mesoscale and marginal sea circulation features can be sampled using along-track altimeter data or trying to interpolate the Sea Level Anomalies (SLA) over a regular two dimensional grid, using all data available from altimeters operating on different orbits. Rather than describing here the various techniques applied to different areas, in what follows we discuss some examples demonstrating the limits of present altimeter systems and the subsequent requirements for future altimeter concepts. However, these requirements can be assumed as ‘optimal’ requirements for the monitoring of all mesoscale and sub-basin scale phenomena.

3.1 Use of along track data to study circulation features

Along-track analysis has the advantage of using the full along-track resolution of present altimeters (~7 km), but excludes any possibility to describe the two dimensional structure of the eddies and precludes the observation of the eddy when it is positioned between tracks. Chance of missing mesoscale eddies using one or even two altimeters in combination are not negligible, mainly in areas where mesoscale is smaller and more rapidly varying, but also when considering larger sub-basin features, as in the case described below.

Figure 3.1 illustrates a typical situation that can frequently happen in a marginal sea like the Mediterranean Sea when the spatial scale of sub-basin field structures are sampled with a single 10 days repeat cycle altimeter as T/P. The AVHRR of figure 3.1 clearly illustrate the space structure of the main dynamical features that characterize the Levantine Basin upper ocean circulation (Malanotte-Rizzoli et al. 1999).

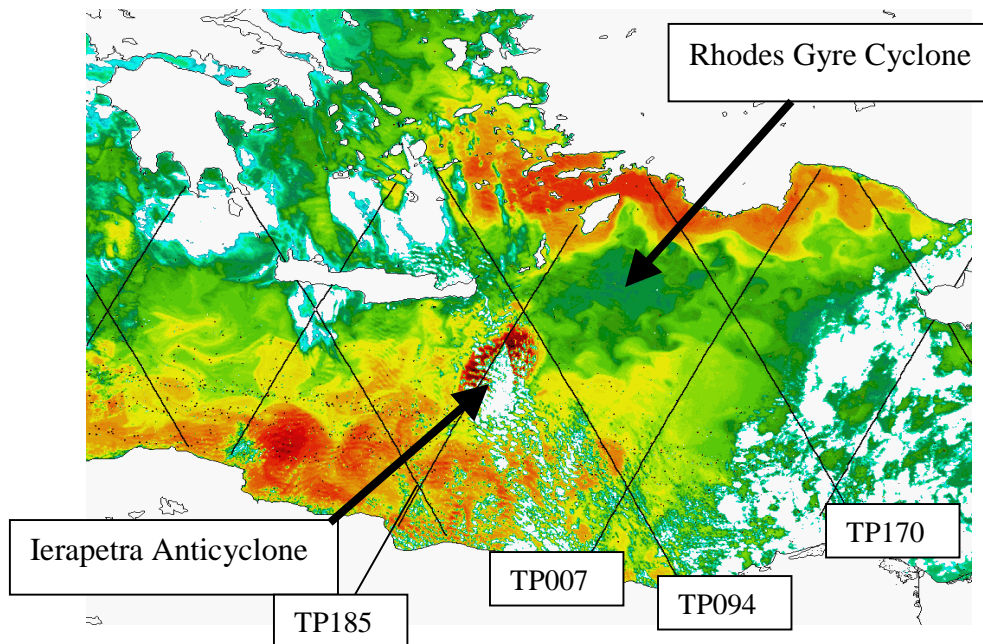


Figure 3.1. AVHRR thermal image of the Levantine Basin (East Mediterranean Sea) on February 22nd 1995. Solid lines indicate the Topex/Poseidon tracks for a ten days window.

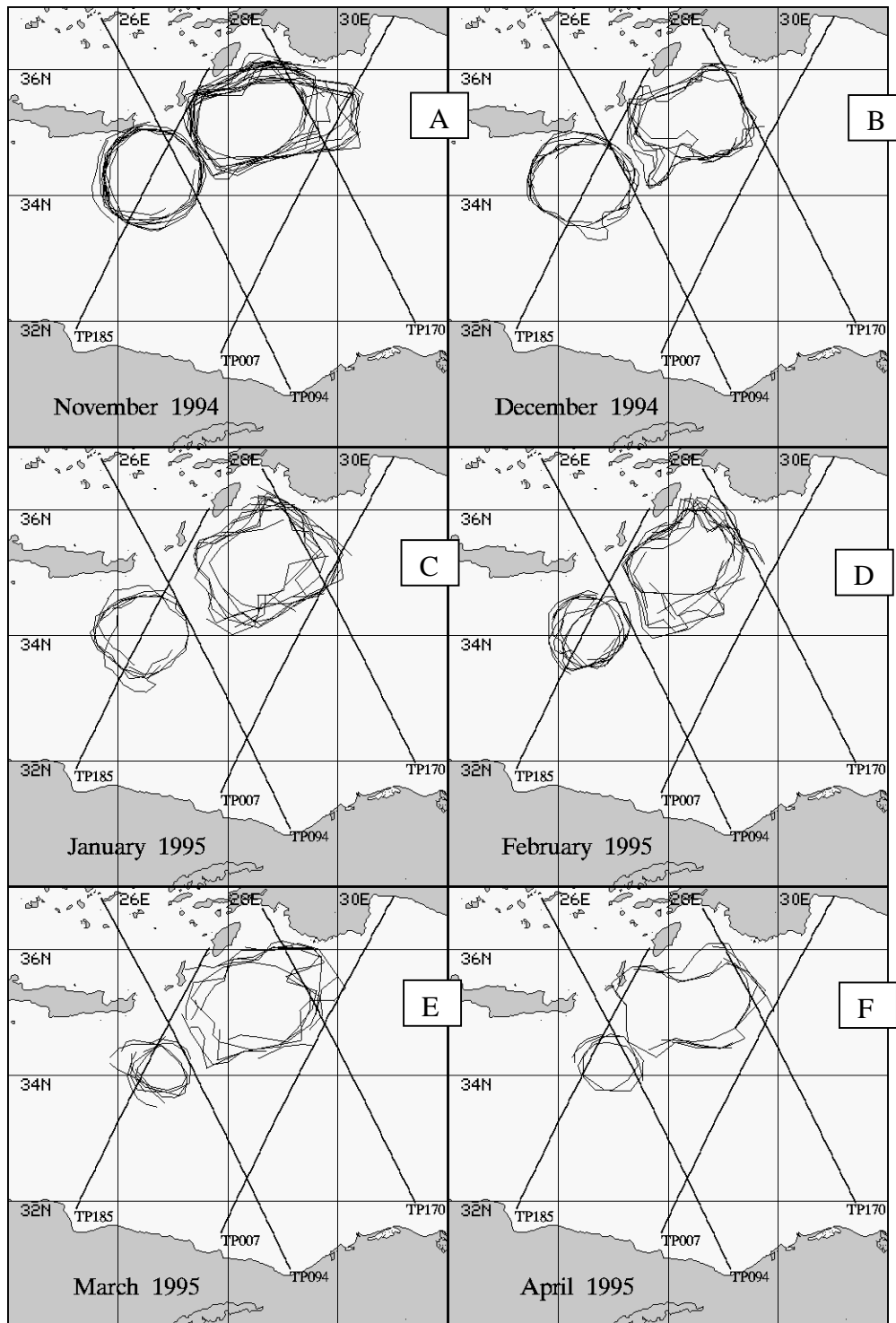


Figure 3.2. Spaghetti diagram tracking the Rhodes Gyre cyclone and Ierapetra Anticyclone from Autumn 1994 to Spring 1995. T/P tracks are superimposed (from Marullo et al., 2002)

It appears evident from figure 3.1 that, while the Ierapetra anticyclone is well sampled from track 185, the Rhodes gyre is completely missed from the altimeter seating

between tracks 185, 007, 094 and 170. The particular situation depicted in figure 3.1 is not just an exceptional case as demonstrated by the 7 months analysis of combined AVHRR and altimeter data illustrated by Marullo et al. (2002). Figure 3.2 shows a so called *spaghetti diagram* that summarizes the evolution of the two gyres from autumn 1994 to Spring 1995 grouping by month the digitalized boundary of the two gyres. In November 1994 (fig 2xa) as well as in October, Ierapetra is visible in all the AVHRR cloud-free scenes. The warm core eddy has a perfect circular shape with a diameter of 80-85 km and occupies the region immediately southeast of the Crete Island. At the same time the Rhodes Gyre have an elliptical shape with a major axis of 100-120 km often oriented in the southwest to northeast direction and a minor axis of ~80 km. A similar situation is seen up to the end of April (figs from 3.2a to 3.2f), when Ierapetra moved southeastward resulting only partially sampled by the altimeter.

The analysis of the Sea Level anomaly time series along T/P tracks 185 and 094 confirms the variability of the Ierapetra position (figure 3.3) showing that Ierapetra disappears from track 185 by the end of March to appear again on track 094 in April 1995.

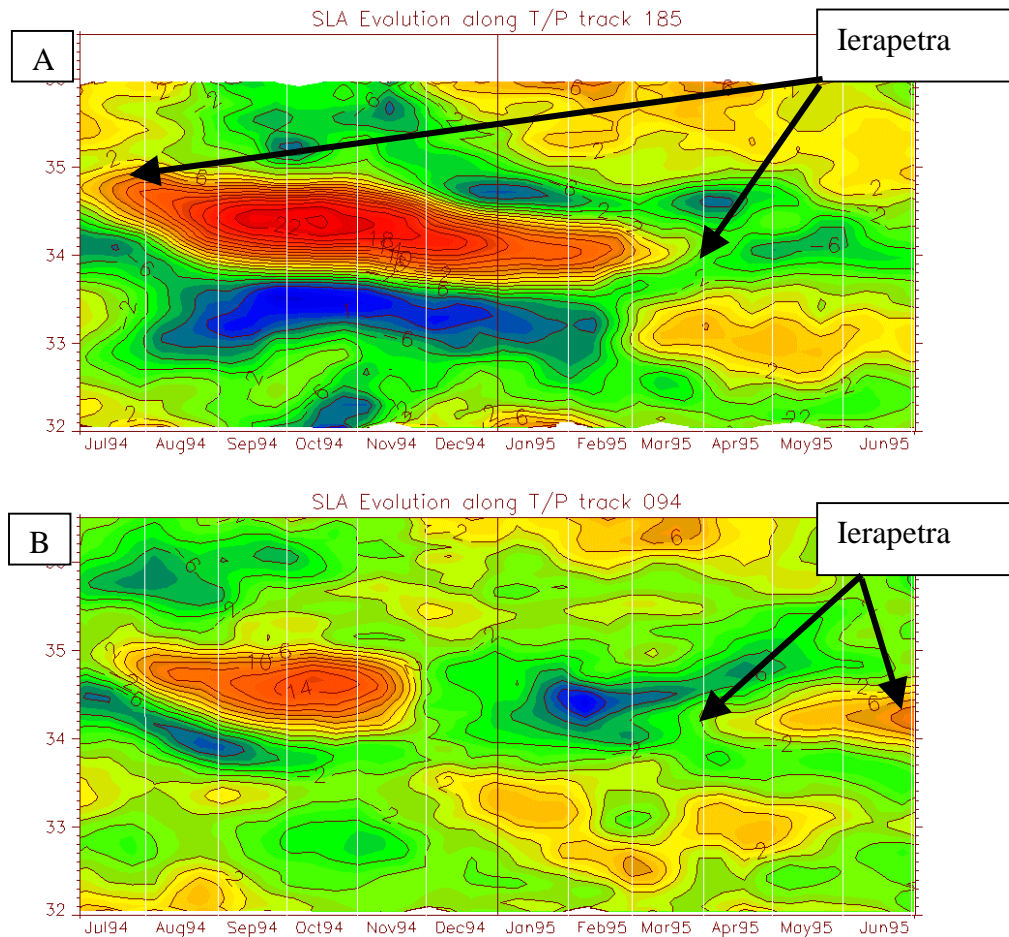


Figure 3.3. Topex/Poseidon Sea Level Anomaly from June 1994 to Jun 1995 along T/P track 185 (A), 094 (B). (from Marullo et al., 2002).

During the same period the presence of the Rhodes gyre is only partially detected by track 170 (fig. 3.4) as a weak negative anomaly from July 94 to April 1995 with absolute minimum in December June.

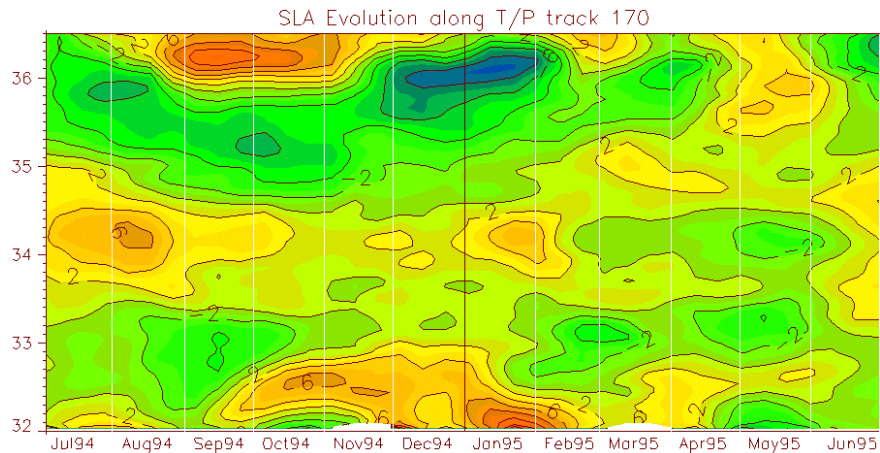


Figure 3.4. Topex/Poseidon Sea Level Anomaly from June 1994 to Jun 1995 along T/P track 170. (from Marullo et al., 2002).

The just mentioned Mediterranean case elucidates two fundamental problems that occur sampling the ocean surface with a single altimeter.

First of all, it appears evident that present altimeters *along-track spatial resolution* is high enough to resolve the open ocean mesoscale or sub-basin circulation. Secondly, they are *able to detect SLA signals associated to weak energy regions* like the Mediterranean Sea (the accuracy would be better increased to 1-2 cm, however keeping it as high as ongoing T/P and ERS one). Problems occur when trying to describe the two-dimensional structure of the SLA field, either because the distance between adjacent tracks is larger than the spatial scale of gyres to be sampled (excluding the possibility to describe the spatial structure of mesoscale features) or because it is not unlikely to miss important gyres that often remain between tracks (the Rhodes gyre is a good example).

The use of more than one altimeter could improve the sampling of mesoscale features if repeat cycles and orbits shifts are well designed. An improvement in this direction can be obtained combining ERS and Topex data (and eventually Jason or other altimeters of future generation). As an exercise it would be interesting to investigate the impact of the additional coverage offered by ERS in the above described area during a ten days T/P period. Figure 3.5 shows the ERS coverage of the area during 10 days. It appears evident that the addition of a second altimeter is still not enough to sample the two gyres on time scale of the order of ten days. In fact, Ierapetra anticyclone results not sampled at all by ERS during the second ten days period and, during the first and third ten days, the two tracks that intersect the gyre do not substantially add more information respect the two T/P tracks 185 and 094. Similar considerations apply for the Rhodes gyre.

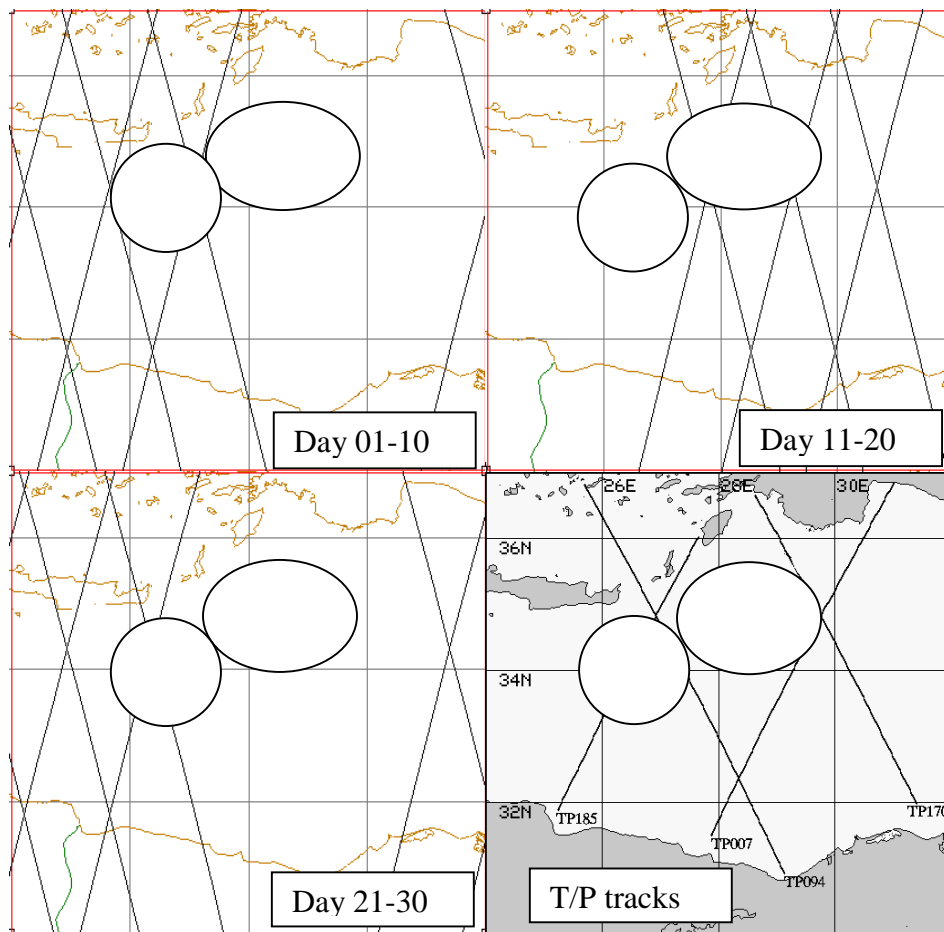


Figure 3.5. ERS tracks for three 10 days T/P cycles in the LIWEX area. The ellipses and the circles indicate the mean position of Rhodes Gyre and IeraPetra respectively.

As already mentioned, the sampling of mesoscale dynamics with altimeter data is a problem also outside the Mediterranean Sea. Figures 3.6 and 3.7 show the difficulty to reproduce the mesoscale features observed by AVHRR using a combination of ERS2 and Topex/Poseidon data.

After 10 days of measurements, ERS-2 and Topex/Poseidon show the presence of the Gulf Stream, but no indications of the mesoscale eddies visible in the AVHRR image are present.

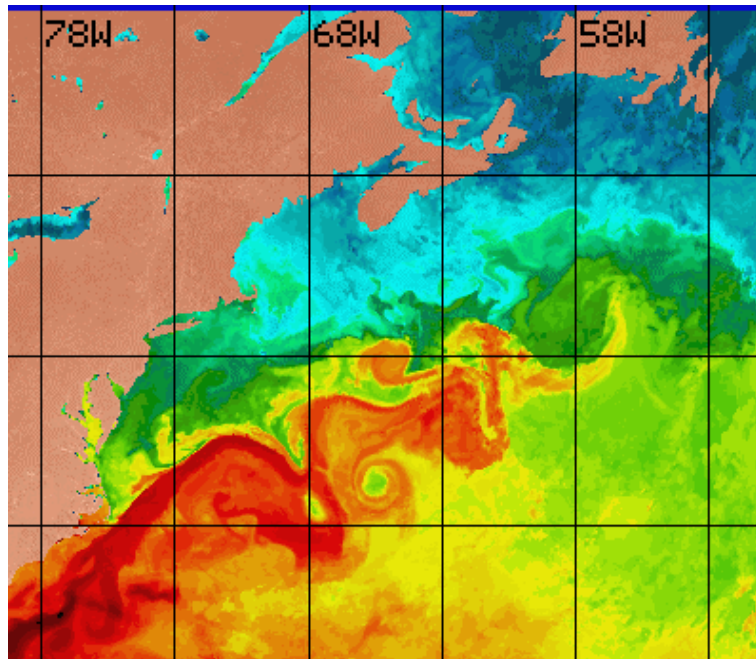


Figure 3.6. AVHRR SST image of the Gulf Stream

*Topex, ERS-2 and GFO Sea Level Deviation (cm) Wrt 1993-95
Apr 20-29, 2002*

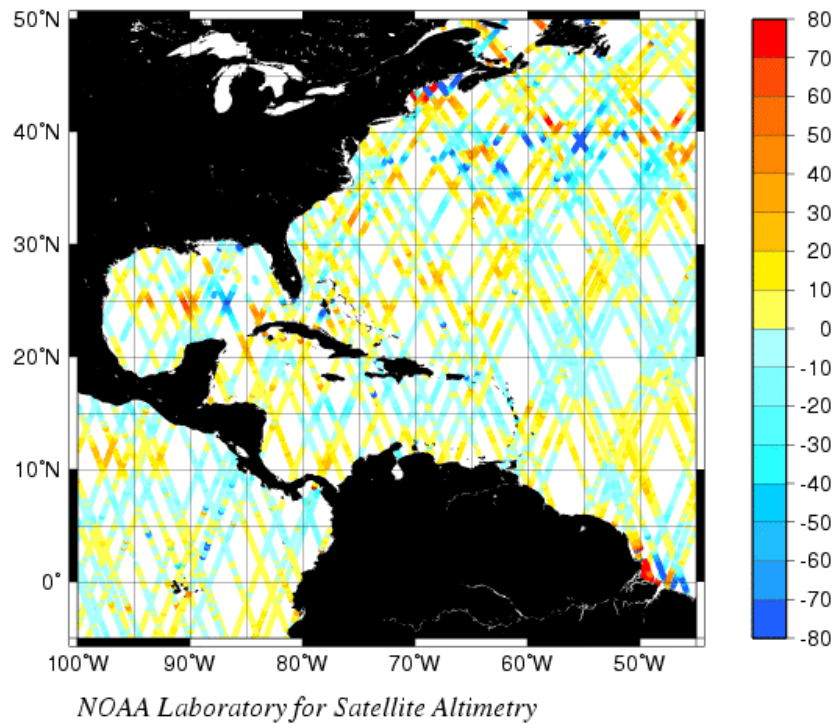


Figure 3.7. Ten days of combined ERS and Topex/Poseidon data in the Gulf Stream Region. (from http://ibis.grdl.noaa.gov/SAT/near_rt/topex_gulfstream.html)

3.2 Mapping of altimeter data

On the other hand, mapping altimeter data over a two-dimensional domain only slightly improves the possibility to describe the two-dimensional structure of the eddy field, as additional problems are related to the interpolation method and, if more than one altimeter is used, to the intercalibration of the different data sets. For most analyses of altimeter data, it is necessary to interpolate the irregularly sampled measurements to map the sea surface height (SSH) field in regular space-time grid. A large variety of mapping algorithm has been applied to altimeter data. The objective mapping based on the Gauss-Markov theorem that minimizes the mean square error of the estimates is often preferred because it is considered the best method of mapping irregularly spaced observations. This method takes into account the effect of the measurements errors and provides also an estimates of the error in mapping. For SSH fields constructed from altimeter data, measurements errors are generally less important than sampling errors due to the irregular space and time distribution of the data (Wunsch 1989).

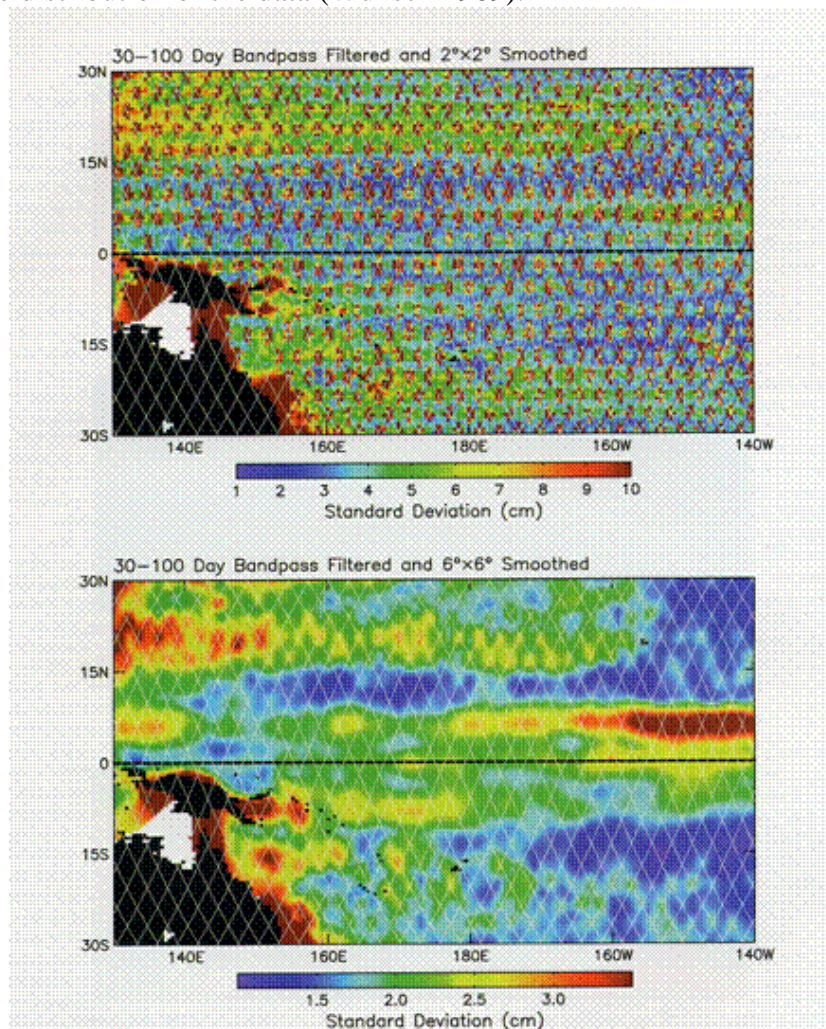


figure 3.8 standard deviation of 7 years of T/P SSH mapped applying a high resolution smoothing algorithm that retained wavelengths longer than 2° longitude and 2° latitude and periods longer than 30 days (upper panel) and with low resolution spatial smoothing algorithm of $6^\circ \times 6^\circ$ and the same 30-100 day bypass filter in time (lower panel)

The key issue is to choose an appropriate degree of smoothing. Several examples can be found in literature that try to show how mesoscale variability can be resolved in altimeter mapping, nevertheless this cannot be done with acceptable accuracy (Greensland et al., 1997; Le Traon and Dibarboure, 1999). For T/P sampling pattern, the mapping errors are spatially inhomogeneous owing to the coarse longitudinal spacing of the ground tracks. The short 10-days repeat cycle implies that the error mapping is homogeneous in time. The pattern of the error for ERS is more complex. The errors are smaller at some locations and times because of the closer spacing of ground tracks but are inhomogeneous in temporally because of the long repeat period.

The limitations of interpolating altimeter data was illustrated in a review of Chelton et al. (2001), mapping SSH fields for a region of the western central pacific, an area in which a variety of dynamical processes are present.

To put in evidence the effect of the undersampling of open ocean mesoscale variability, Chelton computed the standard deviation of 7 years of T/P SSH mapped applying a high resolution smoothing algorithm that retained wavelengths longer than 2° longitude and 2° latitude and periods longer than 30 days (fig. 3.8a, upper panel) and with low resolution spatial smoothing algorithm of $6 \times 6^\circ$ and the same 30-100 day bypass filter in time (fig. 3.8b, lower panel). In figure 3.8a the SSH is characterized by a large standard deviation at the cross-over points and the 3 regions of high variability appear as zonal bands of variability of 5-7 cm, in which patches of high variability are present in correspondence to the crossover points. This systematic geographical variation of SSH variability field is a clear indication of spurious variability due to the inadequate smoothing applied to the data that creates errors in the map. The analysis of the error maps reveals that larger errors occur exactly at the cross-over points, where the $2 \times 2^\circ$ smoothing do not allow to use data far away from the cross-over. When the $6 \times 6^\circ$ smoothing is applied, the spurious large SSH values at the cross-over are no longer present and the bands of high variability are more clearly visible in the map. Even with this large degree of smoothing, there is evidence of sampling errors due to unresolved mesoscale features. In fact, north of 15° patches of high variability are again visible in correspondence of the cross-over points.

The dependence of the pattern of the mapping errors on the smoothing applied to the data was investigated by several authors for the different sampling of the various satellites. Greenslade et al. (1997) proposed to evaluate the adequacy of the smoothing by means of two criteria: the average and the variability of the expected mapping errors over the spatial and temporal grid points at which SSH is estimated. Actually, the effect of sampling errors on mapping SSH/SLA has already been quantified also for merged data from couples or triplets of altimeters (see Chelton and Schlax, 2001). What is found clearly indicates that even merging T/P-Jason-Envisat, in order to keep the error around 2-3 cm, the spatial and temporal resolution cannot be increased to more than 2.5° of longitude and 20 days, which is clearly not enough to resolve mesoscale features or variable sub-basin structures even at mid-latitude.

3.3 Summary of requirements

In principle, to correctly map mesoscale and sub-basin features one would need a distance between tracks of the order of about one third of the baroclinic Rossby radius of deformation that means ~10-15 km for the open ocean and even less for marginal seas like the Mediterranean Sea and for smaller mesoscale (see also the following section). In practice, most of the ocean mesoscale features have dimension of some times the Rossby radius. As a consequence, the optimal spatial resolution needed to resolve these circulation features is 25-30 km cross-track, keeping 10-15 km along track (same resolution required for eventual *imaging* systems), while threshold values would be 30-40 km and 15-20 km, respectively. Corresponding temporal sampling should reasonably attain around 10 days.

All the requirements are detailed and summarized in table A (appendix).

4. Measuring small scales: sub-mesoscale structures and coastal processes

As it has already been observed also in the previous section, mesoscale structures, such as eddies, filaments, frontal instabilities etc., are energetically dominant over most of the world's ocean (Robinson, 1983). Actually, their local dynamics, that was the object of many studies of physical oceanography, still needs investigation, while numerical model simulations indicated that the variability at the scale of internal Rossby radius of deformation plays a fundamental role in the general circulation of the oceans (Haidvogel, 1983; Holland et al., 1983). In a wider context, the knowledge of the eddy transport of momentum in eddy-mean-flow interactions and of the meridional transport of heat through mesoscale features, such as eddies and dipoles, certainly has important consequences also on the possibility to understand better the Earth climate variability.

On the other hand, transient mesoscale and sub-mesoscale features are known to have significant impact on the marine ecosystem functioning. In particular, primary production is modulated by eddies and instabilities through the generation of large vertical motions and changes in the depth of the mixed layer. In fact, global scale marine ecosystems have been characterized according to the photic layer dynamics, the upward flux of nutrients and the seasonal cycle (Longhurst 1995). For all of them the assumed time scale of variability is seasonal. The often observed discrepancy between biomass concentration and seasonal scale mechanisms for sustaining primary production (e.g. pycnocline formation, upwelling, etc.) is generally attributed to short-term intermittent phenomena. Most of them fall in the class of submesoscale-to-mesoscale dynamics (order of 10 km to 100 km) that contains a significant part of the kinetic energy of the ocean (e.g. McGillicuddy Jr, Robinson et al. 1998; Oschlies and Garçon 1998). Understanding and modelling the coupling between mesoscale structures and biota distribution and production is becoming a key issue in marine science (Williams and Follows 1998) as well as in resource assessment management (Huntley, Zhou et al. 1995). Advection, both horizontal and vertical, by small scale structures can transport, and disperse, nutrients and organisms vertically and horizontally enhancing or depressing their impact on the overall carbon flux.

In this context, altimeter data already gave important results, providing fundamental quantitative information on the eddy kinetic energy associated to the upper-ocean current system and on the correlation of EKE with the mean currents (e.g. Iudicone et al., 1998; Larnicol et al., 2002; Morrow et al. 1994; Wilkin and Morrow, 1994). Moreover the variations of the eddy energy at seasonal to interannual scales was provided for the first time on global scale. In addition to this, the frequency/wavenumber spectrum of larger mesoscale circulation could be characterized for each area of interest. However, the characteristics of the time-space sampling of existing satellite systems strongly limits the possibility to monitor open ocean small/sub-mesoscale features at the high level of accuracy that would be required also for a better assimilation into circulation models.

As we move toward the coastal area, the monitoring of small circulation features becomes even a more basic requirement both for science and operational purposes. In coastal and shelf regions, the spatial scales approach a few kilometers and the physical processes are complicated by stronger couplings between different dynamical

phenomena, associated to tidal currents, wind-driven circulation, upwelling and downwelling, local instabilities, inertial and topographically-trapped features, filaments, bottom boundaries, etc. (see, as an example, the results presented at the COAST Meeting in Feb. 2002). However, an operational use of coastal oceanography would have strong impact on several human activities (from fishing to recreation, transportation, etc.) and would certainly aid policy makers/end-users for a sustainable exploitation of marine resources in the coastal areas, also allowing to monitor inshore/offshore exchange of nutrients and pollutants with the open oceans.

Definitely, many of these coastal/shelf processes are characterized by very short spatial and temporal scales that probably will not be resolved even by innovative radar altimeter systems. Anyway, as we will see in the following, an increased sampling, reaching 10-15 km scale, would represent a step forward providing information on nearshore mesoscale processes and improving the nowcast and forecast of the circulation through assimilation in numerical models. All of this would be crucial for our understanding of the coastal ocean circulation and its interactions with the marine environment.

Given this perspective, the questions we will try to address in this section are in some sense quite simple: what are the sampling characteristics of an altimeter system needed to monitor coastal and small mesoscale processes? Or, equivalently: what are the spatial and temporal scales of these processes and their effect on sea surface elevation?

In the following, a few examples based on previous works in the field and on results found in literature will be shown. Obviously, what is described here can not be considered exhaustive, given the high number of processes occurring at the scales of interest, and the different regional responses. In addition, eventual limits/future improvements in altimeter data corrections and retrieval algorithms will not be included in this discussion, being beyond the scope of this workpackage. In any case, it can be observed that a final assessment of the requirements reasonably lies within a factor of about 2.

4.1 Altimeter accuracy

The first Altimeter/Synoptic Mesoscale Plankton Experiment (ALT/SYMPLEX 1996) was specifically designed to perform in situ measurements simultaneous with the passage of TOPEX/POSEIDON (T/P) and ERS 2 (Buongiorno Nardelli et al., 1999). Direct comparison between SLAs and dynamic heights was made along selected altimeter tracks in the central Mediterranean through the computation of dynamic heights from CTD (Conductivity Temperature Depth) density profiles. This experiment made it possible to have, for the first time, a validation of altimetry with in situ data in an area where a weak dynamics results in modest sea elevations, rarely exceeding 10 cm (typical conditions observed in semi enclosed seas). A good agreement was found between SLAs and dynamic heights (fig.4.1). The correlation between the different profiles ranged from 0.72 to 0.89. Looking at the simultaneous SST map derived from AVHRR (fig.4.2), we can observe that T/P track 059 in April detected a cold filament that is wrapping around and forming a hammer-like structure (actually the dominant feature is a cyclonic eddy centered at 35.5°N, 13.2°E), with a horizontal scale of ~ 40 km. The comparison between SLA and simultaneous in situ dynamic heights derived from CTD density profiles thus substantially demonstrated that T/P and ERS-2 sensors are adequate to detect also small

mesoscale signals. Consequently, in order to monitor submesoscale-to-mesoscale features, the accuracy of any future altimeter system basically needs to be at least equal to that of ongoing altimeter missions T/P and ERS, even if most of the ambiguity in the interpretation of the data would be removed increasing it to 1-2 cm.

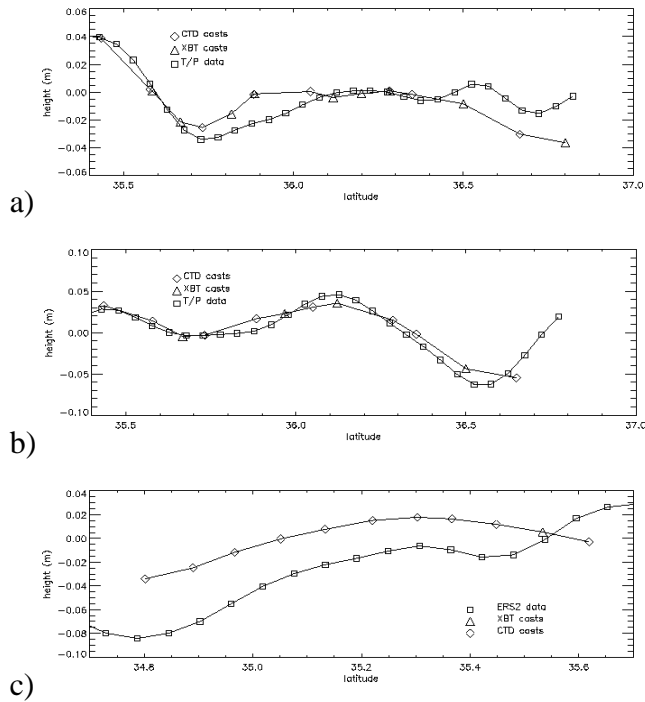


Figure 4.1. Sea level anomalies and dynamic heights along T/P 059 (16 April (a); 6 May (b)), and ERS-2 079 (5 May (c)) tracks.

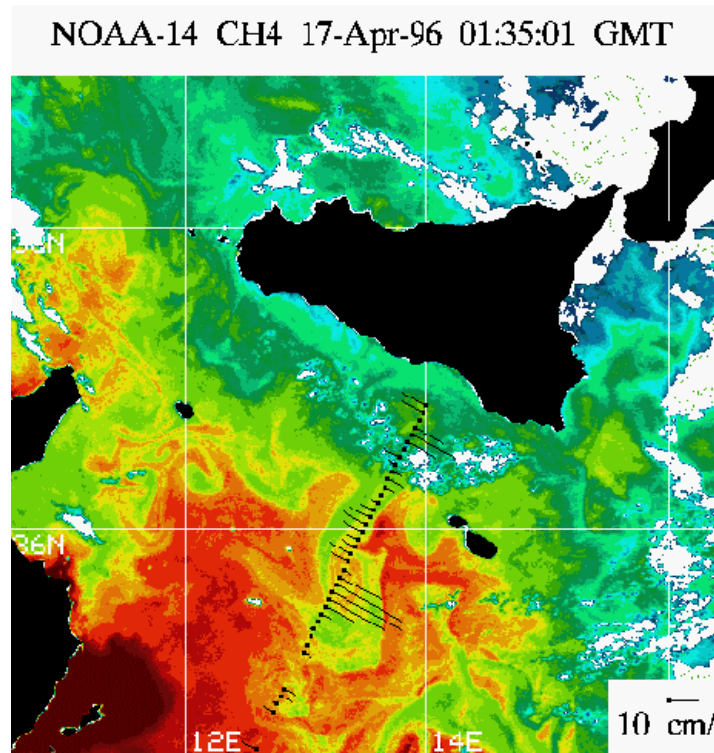


Figure 4.2. NOAA-14 ch.4 image (17 April 1996) with T/P track 059 velocities (16 April 1996).

4.2 Temporal and spatial sampling

In recent years, many studies have been conducted on the internal instabilities of upper ocean fronts and on the processes by which water is transferred into the stratified ocean interior. This mechanism, generally referred to as subduction, rules the absorption of chemicals from the atmosphere by the ocean and has relevant consequences both on the climate system and on the biological activities. Actually, numerical studies, that demonstrated that strong subduction is associated to frontogenesis and baroclinic instabilities, found confirmation in experimental data collected in different areas around the world (e.g. Samelson and Chapman, 1995; Spall, 1995, Allen and Smeed, 1996).

In particular, Spall (1995) configured a simple numerical model (three isopycnal layers) to approximate the fronts observed in the North Atlantic Convergence Zone during the Frontal Air-Sea Interaction EXperiment (FASINEX) and found that strong vertical motions are associated to the perturbations that grow in amplitude through baroclinic instability. From his experiments, and coherently with the observations, the horizontal scale of the vortices that separate from the front is ~ 25 km in diameter, while the time needed for the instability to grow and detach is ~ 2 -3 weeks (see figure 4.3).

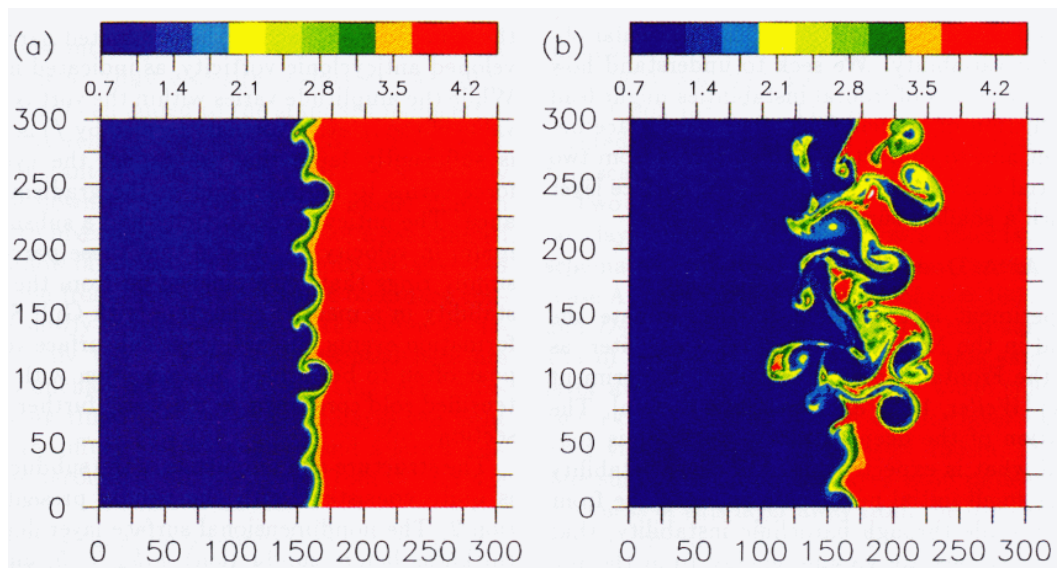


Figure 4.3. Potential vorticity on the subducting layer (isopycnal layer 2) a) at day 8 of integration b) at a later stage on day 24.

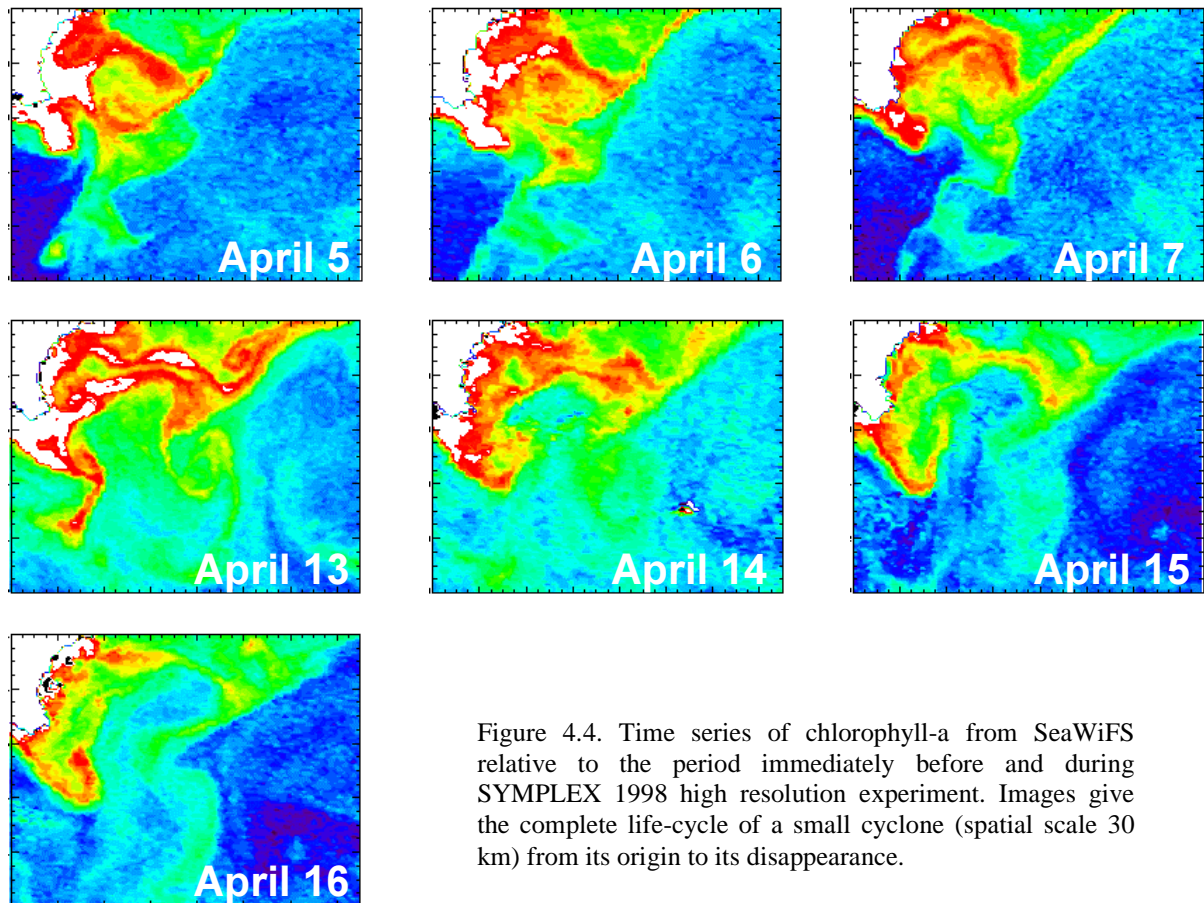
A second example is given by the data collected during the third SYMPLEX experiment (1998). SYMPLEX 1998 included an high horizontal resolution experiment aimed to characterize from a dynamical point of view a small mesoscale eddy (~ 30 km in diameter) that was observed off the coast of Sicily island (Mediterranean sea). This small cyclone was shown to develop from a coastal filament in SeaWiFS chlorophyll images.

In figure 4.4 we can see the time series of chlorophyll-a from SeaWiFS relative to the period immediately before and during the experiment. Unfortunately cloud coverage did not allow a continuous monitoring of the area. Anyway, the available images give the complete life-cycle of the small cyclone from its origin to its disappearance. In all the

images a quasi-stationary wavelike meandering of the surface flow is marked by the maximum chlorophyll concentrations.

On April 5 the higher chlorophyll is confined in an almost round area east of southern tip of Sicilian coast. A general anticyclonic circulation seems to characterize this water. In the following image a small portion of water rich of chlorophyll begins to detach and gradually acquires cyclonic vorticity. This feature is well identifiable on April 7th as a spiralling eddy with a radial dimension of the order of few kilometers. By April 13, the eddy is still characterized by two spiraling filaments, one connected to the coastal chlorophyll maximum, one extending to the south. Its dimensions have now reached the mature state, and the day after the cyclone closes on itself. On April 15 the small cyclone is still visible with higher values of chlorophyll, however it is almost disappeared by April 16.

In conclusion, this mesoscale eddy originated within the maximum of chlorophyll marking the meandering northeastern surface flow, developed to a mature phase, and started to decay in about 10 days.



SYMPLEX-3 high horizontal resolution survey data allowed a complete dynamical characterization of the eddy through assimilation of CTD data in a numerical diagnostic model for the ageostrophic components of the flow (see fig.4.5 as an example), showing vertical velocities reaching up to 15 m d^{-1} (Buongiorno Nardelli et al.2001).

Hydrological sampling was chosen to be less than 10 km (see figure 4.5), in order to resolve the main features without losing a quasi synoptic view of the instability (CTD measurements lasted from April 12 to April 16 1998).

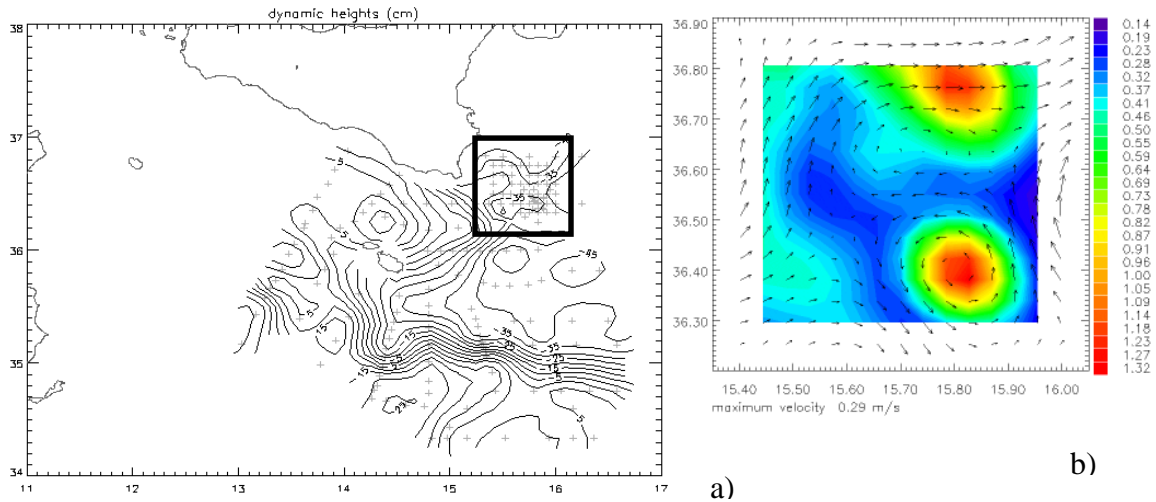


Figure 4.5 (a) Dynamic heights from in situ data in the area of the SYMPLEX-3 experiment (crosses indicate in situ measurements); (b) potential vorticity and geostrophic velocities from assimilated data in the sub-mesoscale eddy studied during the high resolution experiment .

4.3 Summary of requirements

Actually, coastal currents and open ocean small mesoscale features have similar temporal and spatial characteristics. All the examples provided above show that studies on small/sub-mesoscale and coastal processes require an isotropic horizontal spatial sampling ranging between 10-15 km, with a repetition of the measures that should achieve 3-5 days, while accuracy should at least remain the same as those of T/P, better if increased to 1-2 cm. However, near the coasts additional problems are related to the unknown and amplified tidal signals (tide/topography interaction). High spatial resolution altimetry (spatial sampling up to 5 km, according to Le Provost, 2001) could help the mapping of tidal characteristics provided that long timeseries of data are planned and if a proper aliasing of tidal signals is chosen.

All the requirements discussed in this section are summarized in table A (appendix).

5.Operational oceanography

The vital importance of a rapid dissemination and systematic assimilation of observational data into numerical models in order to provide forecasts of the state of the seas, oceans and atmosphere, better referred to as *operational oceanography*, has been recognized since 1990 by the GOOS (Global Ocean Observing System) international programme.

Actually, operational oceanography consists of a complex system, involving the rapid transmission of measurements to data assimilation centres, and the rapid release of nowcasts, forecasts and hindcasts through high-level computational resources. The result is a real time (or near-real time) accurate description of the present state, together with a forecast of the future conditions of the sea. Many advantages come from operational oceanography, as the possibility to assemble long term data sets that can help the description and interpretation of past states, and time series showing trends and changes. Moreover, the outputs from operational models can be used to generate additional data products, often through intermediary value-adding organisations, that include warnings (of coastal floods, ice and storm damage, harmful algal blooms and contaminants, etc.), electronic charts, optimum routes for ships, prediction of seasonal or annual primary productivity, ocean currents, ocean climate variability etc. Forecasts of the state of coastal seas and oceans for days to decades into the future will add significant economic benefits, supporting and improving the performance of existing maritime industries and services.

In this context, satellite altimetry obviously represents one of the most promising means to define the dynamical state of the oceans for operational purposes. Consequently, since the promotion of the European contribution to the GOOS (EuroGOOS) in 1994 (Fisher and Flemming, 1999; Bosman et al., 1998, Prandle and Flemming, 1998), various projects used satellite altimetry as one of the main sources for near real time (NRT) analysis and assimilation in numerical models. In particular, altimeter data were assimilated weekly during the MFSPP (Mediterranean Forecasting System Pilot Project), funded by the EU-MAST Project for the Mediterranean Sea, and their use is under development for the European Atlantic forecasting systems (DIADEM,FOAM, MERCATOR). In this section, some details on the MFSPP system, as an example of an operational forecasting system, will be given. This will allow to define some possible/necessary improvements for the future observing systems.

5.1 Mediterranean Forecasting System Pilot Project

The Mediterranean Forecasting System (Pinardi and Flemming, 1998; Pinardi et al., 2002) established two major goals:

Scientific: to explore, model and quantify the potential predictability of the ecosystem fluctuations at the level of primary producers from the overall basin scale to the coastal/shelf areas and for the time scales of weeks to months through the development and implementation of an automatic monitoring and a nowcasting/forecasting modeling system, the latter called the Mediterranean ocean Forecasting System (MFS) as a whole.

Pre-operational: to demonstrate the feasibility of a Mediterranean basin operational system for predictions of currents and biochemical parameters in the overall basin and

coastal/shelf areas and to develop interfaces to user communities for dissemination of forecast results.

These goals should be achieved in three phases:

1. First Phase (1998-2001): a pilot project for the implementation of the observing system backbone and demonstration of forecasting capabilities at basin scale

2. Second phase (2002-2005): consolidation and upgrade of the observing system for the physical components, extension of observations to biochemical variables, demonstration of regional forecasting capabilities for ten days range, three-dimensional ecosystem model implementation

3. Third phase (2006-2008): observing system verification and further extension toward operationality, shelf areas primary producers forecasts, consolidation of products from forecasts.

The coastal environmental prediction problem at short and medium time scales requires the understanding and modelling of the large spatial and long time scales, as well as the local and short scales (Pinaridi et al., 2002). A possible methodological approach is to 'downscale' the large/long scale processes to the local/short scale, hypothesizing a conceptual model that parameterizes the effects of the large scale at local level through nesting of different physics and resolution observations and models.

In general, we may say that the coastal environmental prediction problem can be connected to the design of an interdisciplinary observing system coupled with numerical predictive models of atmospheric, oceanic and marine biochemical state variables. The most important component of the predictive system is the assimilation engine that merges the observations with different predictive state variables trying to reduce the uncertainties associated with the knowledge of the initial condition. However, the coastal environmental prediction problem has a multiplicity of system components that could limit the predictability time. They are: 1) the limited predictability of the atmospheric forcing directly influencing the coastal dynamics; 2) the lateral boundary condition uncertainties, considering both the open boundary conditions and the river runoff uncertainties, affecting the long term memory of the system; 3) the adjustment processes to the downscaling of large scale initial fields; 4) the initial conditions specification for all the dynamical variables of interest; 5) the flow field nonlinearities.

5.2 Assimilation of altimeter data

It is clear that satellite altimetry could strongly improve the environmental prediction capabilities through its fundamental contribution to component 4) in the list above. Actually, even if the sea level is a dynamical variable related to the surface circulation, it also contains information on the vertical structure of the sea, which are not trivially related to the altimeter measurement itself. This remark stimulated a theoretical effort to provide an optimal estimate of the state of the system consistent with the physics resulting from both models and observations, i.e. an optimal methodology for the assimilation of the altimeter data in the numerical models (see for example Fukumori et al., 1993; Ganachaud et al., 1997; Fox et al., 1999; Stammer, 1997).

However, even if data assimilation is an optimal estimation problem in which the nature of altimeter sea level measurements still needs investigation, it is sure that a

fundamental concern is due to the NRT range accuracy and to the sparse time and space sampling of the ocean surface by existing and planned satellite missions.

The NRT SLA used in the framework of MFSPP were produced both along track and on the general circulation model grid. The acquisition system worked on a continuous mode and received all the data necessary from several centres (ERS-2 Geophysical Data Records-GDR from the Global Teleconnection System-GTS, ERS-2 orbit computed by Deft University, Topex and Poseidon Navocean GDR and ECMWF meteorological fields). After the acquisition step, the usual geophysical corrections were applied (wet and dry tropospheric, ionospheric, electromagnetic, tides, inverse barometer, Le Traon and Ogor, 1998). The along track analysis was then completed by the removal of a mean SLA computed separately for ERS-2 and T/P for the period Jan 1993 to Dec 1997. Finally, mapping of along track SLA on the forecasting model grid at 1/8 x 1/8 degrees horizontal resolution was carried out with objective analysis techniques especially developed for the satellite data (Le Traon et al.,1998). Maps were produced every week at time T0-7, using three weeks of data (two before and one after T0). In figure 5.1 an example of the comparison between model SLA after assimilation of the data and a map of SLA from combined T/P-ERS is presented.

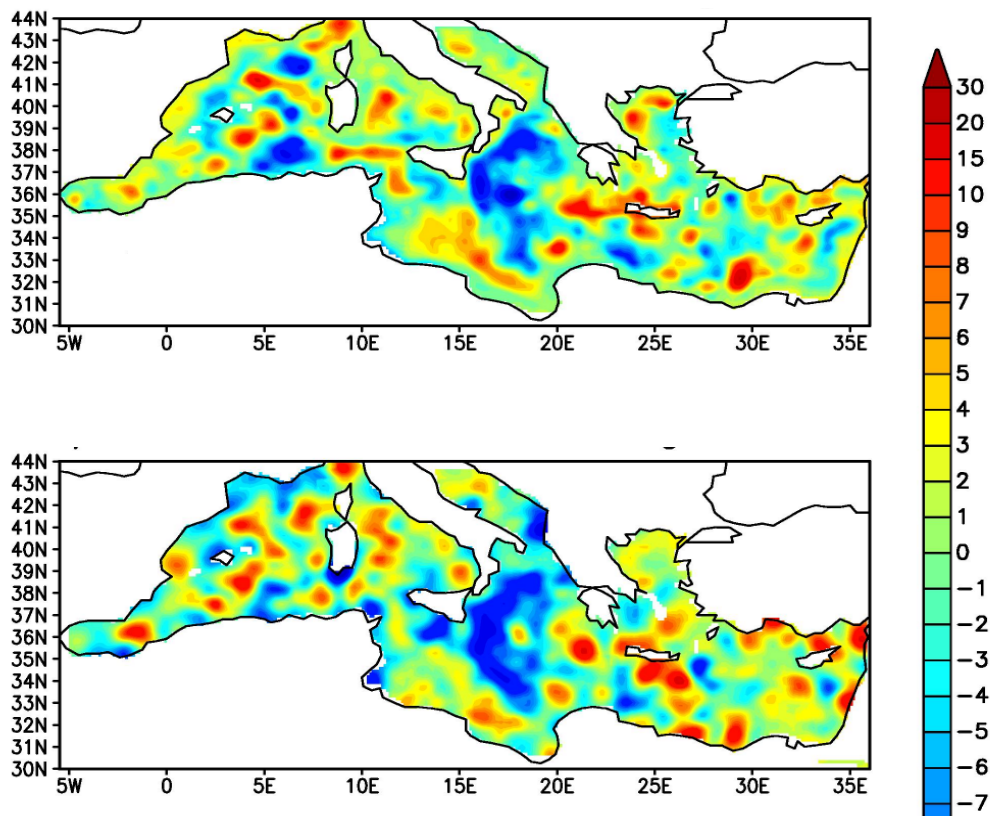


Figure 5.1 (a) MFSP Model analysis of week 14-20 august 2000 after assimilation of along track T/P and ERS data; (b) T/P+ERS2 data objective mapping for the same week.

5.3 Space and time sampling requirements

The nadir-pointing property of altimeters limits spatial sampling in the direction across satellite ground tracks, causing problematic analyses mainly of mesoscale features (see also previous sections), especially if considering a single satellite. In addition, the complex pattern of ground tracks, associated to the near-polar orbit makes difficult also the analysis of large horizontal scales associated to high frequency variability, such as tides and wind-forced barotropic motion.

In figure 5.1, we present a typical three-weeks coverage of the Mediterranean, which was used to produce an analysis. The altimeter data coverage aid to resolve only the large circulation feature, as each two weeks, T/P covers 32 and ERS-2 43 tracks, leaving many areas almost completely not sampled.

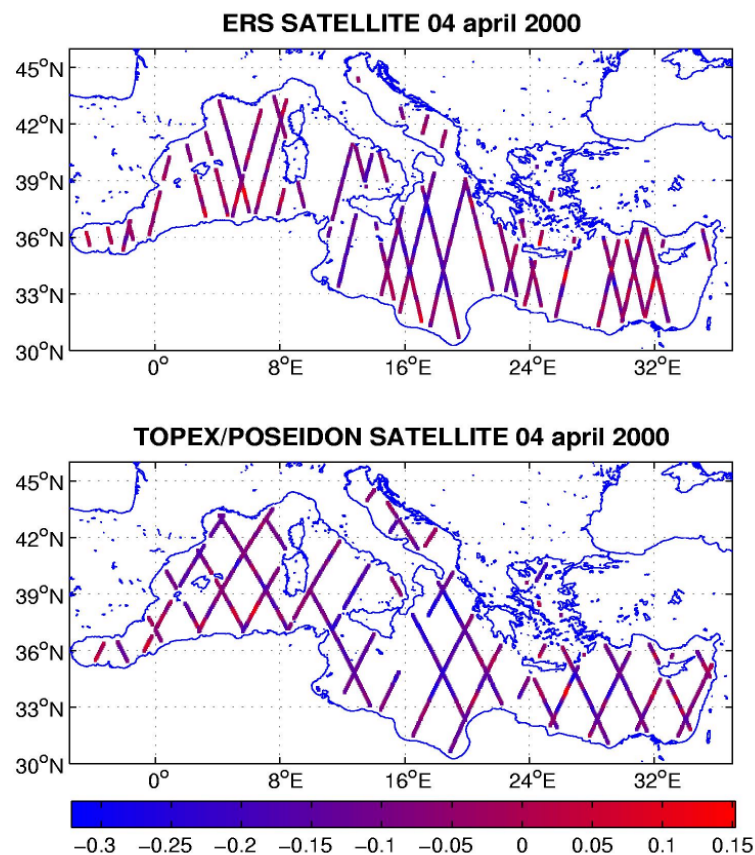


Figure 5.1 The T/P and ERS-2 tracks for a two week period from march 19 to april 2, 2000, used in the assimilation that produced an analysis at April 4, 2000.

It is a natural consequence that a change in space and time sampling is highly recommended (5-10 days repeat time but with ERS-2 coverage would strongly improve the initialisation of the model). Even stronger requirements would be needed for the assimilation in coastal/shelf models. In the best hypothesis, coastal areas altimetry should in fact have wide swath coverage to compete with in situ sea level stations.

5.4 Accuracy requirements

For verification purposes, the NRT maps from T/P and ERS-2 were intercompared with the Delayed Mode (DM) data that are more accurate allowing for a reduction of orbit errors. In fact, the main problem with NRT data was represented by the orbit determination, specifically for ERS-2. In order to reduce this error, the procedures described in Le Traon et al. (1995), consisting in the minimization of the T/P and ERS-2 crossover differences on a time window of 21 days, were applied.

	RMS T0-7	RMS T0-14
Annual statistics		
T/P + ERS-2	3.76	3.30
T/P	3.21	2.49
Winter statistics		
T/P + ERS-2	4.00	3.43
T/P	3.66	2.83
Summer statistics		
T/P + ERS-2	3.36	3.17
T/P	2.53	2.15

Table 5.1. Root Mean Square–RMS of the differences between the NRT and the DM data for the period Sept.1999-Sept 2000. The columns with RMS at T0-7 and T0-14 days correspond to maps done at these different times.

The mean error associated to the NRT system could be estimated by calculating the average for all the grid points of the rms of the differences between NRT and DM maps. Table 5.1 gives the rms error for the combined T/P and ERS-2 maps (TPERS) and for the maps done only with the T/P. For combined TPERS maps the rms is about 3.76 cm and 3.21 cm for T/P maps. This error represents a non-negligible part of the mean variance of SLA (comprised between 6 to 9 cm). The main source of difference between the DM and the NRT data is the orbit error and, to a minor extent, the different amount of data used in the two analyses (the NRT system computes a combined map, every week, using only three weeks of data while four weeks are used for the DM maps). As a consequence, it must be stressed that a precise orbit determination in near real time should have a high priority in any future altimeter mission.

6. Ocean surface winds and waves

6.1 *The measurement of wind speed and wave height*

In this section we discuss the derivation of wind speed and wave height from the altimeter signal, the problems connected, the related applications, and the requirements for a new altimeter system.

The basic quantities to be derived from the altimeter signal are altitude range, wind speed and wave height. The range has been extensively described in the previous sections. Here we concentrate on wind speed and wave parameters. While the range information is derived from the time elapsed between the emission of the signal and the reflected wave reaching the antenna, wind and wave characteristics are derived from those of the return signal. In particular:

wind speed is derived from the intensity of the returned signal with respect to the emitted one. The returned signal depends on the reflective properties of the surface. In turn these depend on the number of wavelets (a few centimetres long) characterising the sea surface. These are linked to the local surface wind stress, and consequently wind speed.

wave height is derived from the time difference between the beginning and the saturation of the return wave signal. The principle is that the reflecting points are distributed along the surface profile of the dominant waves. Therefore the above time difference depends on the height difference between crests and troughs of the waves, which is exactly the wave height we care about.

A further quantity that is presently actively pursued is the **wave period**. This is derived from a combination of wave height, backscatter coefficient and wind speed (Davies and Challenor, 1997).

6.2 *The problems connected to the measurements*

The relation between the altimeter backscatter measurements and the ocean surface properties are however not entirely resolved. They depend on a number of parameters or conditions, whose influence is by no means fully known. Although in general altimeter significant wave height (SWH) measurements have been shown to compare satisfactorily with in situ buoy wave height estimates (Challenor & Cotton, 2001) altimeter wind speeds are known to include residual sea state effects (Glazman & Greyshuk, 1993; Gommenginger et al, 2002a). There is a definite dependence on wave height, or, more precisely, on the mean slope of the sea surface. Young wind sea, i.e. steep waves under active wind generation conditions, are notably rougher than well-developed waves under the same wind speed. This may lead to seasonal and regional biases, as it is clearly shown when comparing altimeter against buoy data in different climatic regions (Figure 6.1). Even recently proposed altimeter wind speed models which include a significant wave height parameterisation (Gourrion et al., 2000) display nevertheless a residual dependence on wave age (Figure 6.2). At the same time, the widely used relation between wind stress and the ocean wave age has been challenged (Taylor & Yelland, 2001) in

favour of a dependence on wave height and wave length, the latter being connected to the wave period, which, as described in the previous sub-section, can be obtained from the altimeter signal. Similarly, the availability of dual frequency backscatter measurements from the Topex altimeter has resulted in a number of studies into the retrieval of for example wind stress (Elfouhaily et al, 1998) or rain rate (Quarty, 1998), using nadir altimeter measurements.

Two different problems concern the low and high ranges of wind speed U_{10} . At low U_{10} values the surface acts as a mirror and the return signal is saturated. This range is relevant for the definition of the conditions in the tropics, an area where the present accuracy of the global meteorological models is lower than elsewhere. At the other extreme, at high wind speeds (> 20 m/s), the present data lose reliability. This is connected to a parallel problem in the measurement of the wave height.

On the high value range the problem is a mixture of physics and characteristics of the altimeter. At very high wind speed, the surface becomes saturated with wavelets (particularly in the early stages of generation by wind), and the surface is covered with spray. As a matter of fact the surface itself becomes less defined in extreme conditions. This is relevant also for the estimate of range, whose accuracy is strictly connected to the one with which we measure the wave height. The point is that during the generation of a storm by wind, the single wave heights in a certain area are not Gaussian distributed, the distribution being skewed towards the crests. This leads to a bias of the range, whose estimate depends on the accuracy of the wave measurement. This point is further discussed later.

Another problem in the use of the altimeter appears in coastal areas, when the instrument is flying offshore. In these cases the instrument requires a few seconds for locking the signal onto the sea surface. This implies that in these cases no information is available in the coastal areas, which is exactly where most of the economical interest is concentrated. An improvement in this respect is strongly needed.

6.3 Global wind and wave climatology: short term applications

One of the main practical applications for the wind and wave data derived from the altimeter measurements is the possibility to produce reliable atlases of wind and wave global conditions. On short term applications, the altimeter wind and wave data provide the essential information for the correction, by data assimilation, of the daily forecast produced by the meteorological and wave models operational at various centres, e.g. the European Centre for Medium-Range Weather Forecasts (Reading, UK). Similarly, in spite of the absence of wind direction information, altimeter winds are used as a global dataset to validate scatterometer-assimilating numerical models (e.g. NCEP and ECMWF).

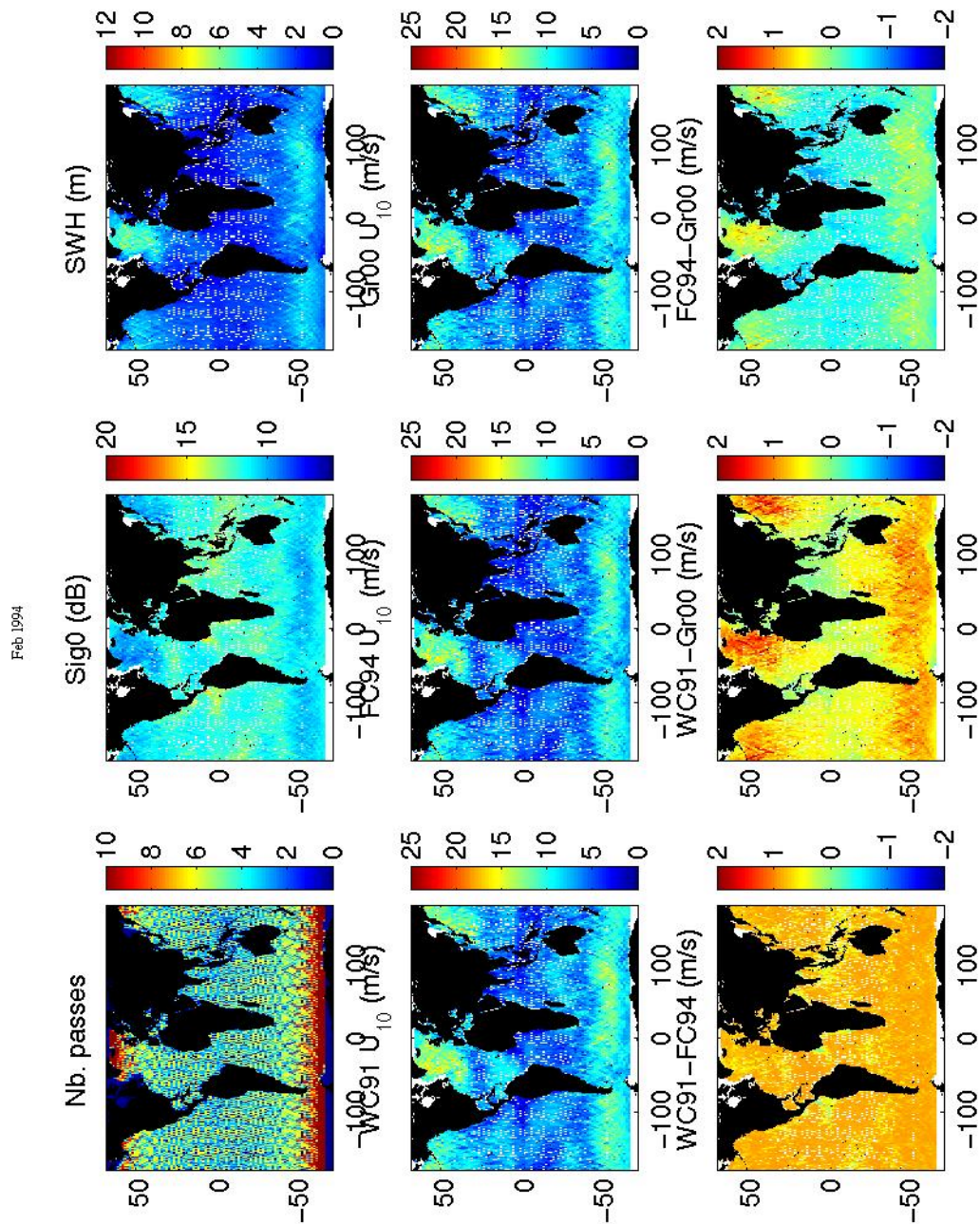


Figure 6.1: Global monthly (February 1994) averaged altimeter wind speed gridded over 1.5x1.5 degree boxes. Subplots from top left to bottom right show respectively (a) number of Topex passes, (b) altimeter backscatter at Ku-band, σ_{Ku}^0 , (c) altimeter significant wave height at Ku band, (d) altimeter wind speed after Witter & Chelton (1991), (e) altimeter wind speed after Freilich and Challenor (1994), (f) altimeter wind speed after Gourrion et al. (2000), (g) = (d) - (e), (h) = (d) - (f), (i) = (e) - (f). In (i), see how the wind speed difference between the σ_{Ku}^0 -only model by Freilich & Challenor and the (σ_{Ku}^0, SWH) model by Gourrion (2000) reaches up to 1 m/s in the monthly mean. This SWH effect is in addition to the wave age effect see in Figure 2.

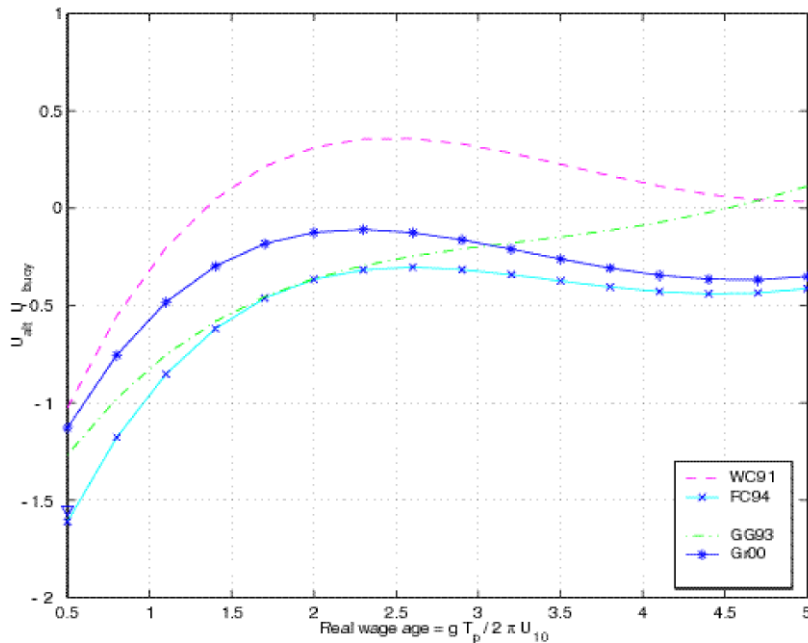


Figure 6.2: Residual altimeter wind speed error against wave age for a number of altimeter wind speed retrieval models. The trend was observed using a dataset of collocated Topex/buoy measurements (Gommenginger et al, 2002a) with available in situ information on wave period.

6.4 Global wind and wave climatology: long term applications

Where long-term altimeter records exist, e.g. the continuous 10 years dataset from Topex/Poseidon, altimeter wind and wave information can serve also to monitor inter-annual and decadal variability of the atmospheric forcing and the response of the ocean. As well as monitoring its temporal variability, the global capabilities of spaceborne altimeters allow also changes in the spatial distribution of the forcing to be detected. Through this, it is possible to associate increased variability in the North Atlantic wave climate to changes in atmospheric patterns. Hence, a substantial rise (up to 0.6 meters) in wave heights of the north-eastern Atlantic during the latter part of the twentieth century is attributable to changes in the North Atlantic Oscillation (Woolf et al., 2002; Figure 6.3)

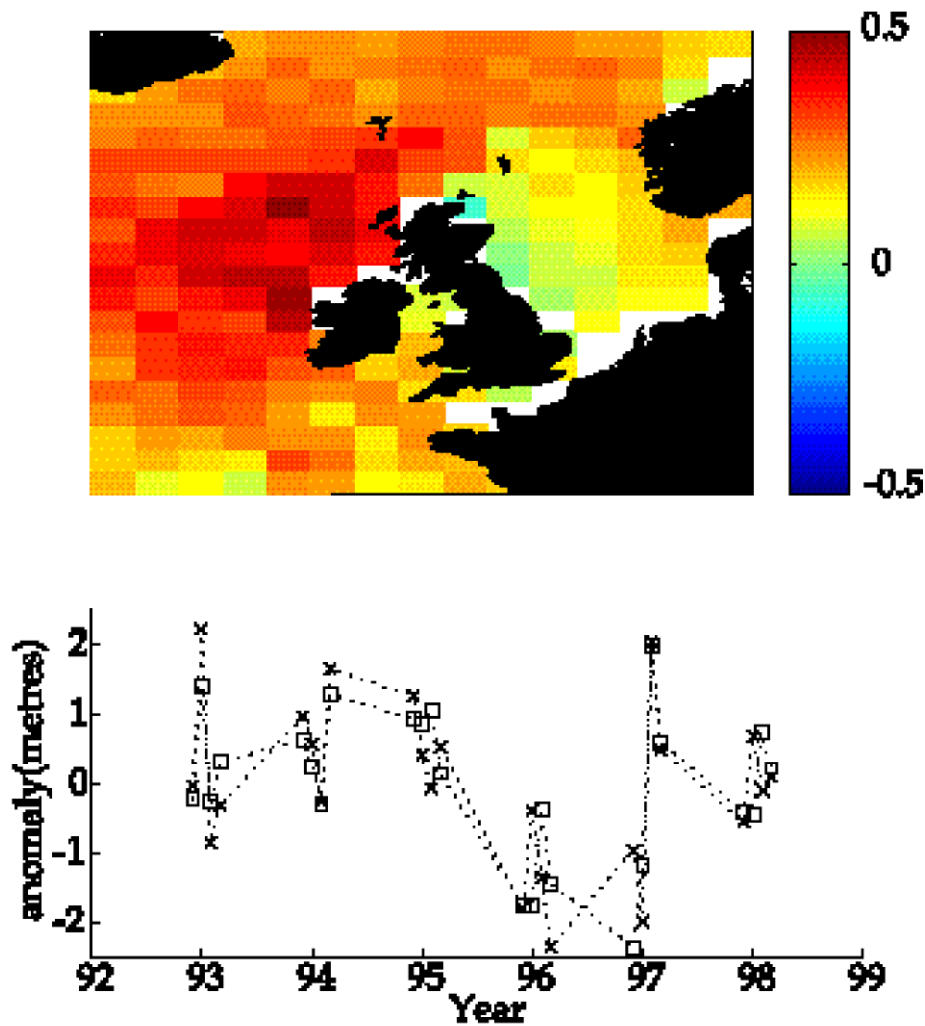


Figure 6.3: The relationship of inter-annual variability in mean monthly wave heights during the winter months (December - March) to the North Atlantic Oscillation. The upper panel maps the apparent sensitivity of mean monthly wave height to the NAO index (units are metres/unit NAO index). The lower panel shows the measured anomaly in wave height (crosses) and that implied by the NAO index (squares) at the edge of the Hebridean shelf (57°-58°N, 8°-10°W).

6.5 Sea State Bias correction

Another, possibly more critical, application of altimeter wind and wave data, lies in the need to correct the altimeter mean sea level measurements for sea state bias (SSB) error. This error is linked to the presence of non-linear ocean waves on the ocean surface and results in the mean sea level over the altimeter footprint being underestimated (Srokosz, 1986). The SSB error is the largest remaining error in the altimeter sea surface height measurements, and can easily obscure genuine ocean circulation feature as the height error can reach several percent of the significant wave height (e.g. 4% of 3 m SWH = 12 cm). This error is currently corrected for in operational altimeters using an empirical dependence on the altimeter wind speed and significant wave height data

(Gaspar et al, 1994; Gaspar & Florens, 1998), although more recent findings relate the SSB error more closely to the surface rms slope (Gommenginger et al., 2002b; Millet et al., 2002; Figure 6.4). But until the measurement of rms slope from altimeter becomes possible (as is suggested by Elfouhaily et al (2002) from the Doppler-delay spectrum in GNSS bistatic configurations), it is essential to ensure that wind speed and significant wave height measurements, collocated with the altimeter range measurements, remain available.

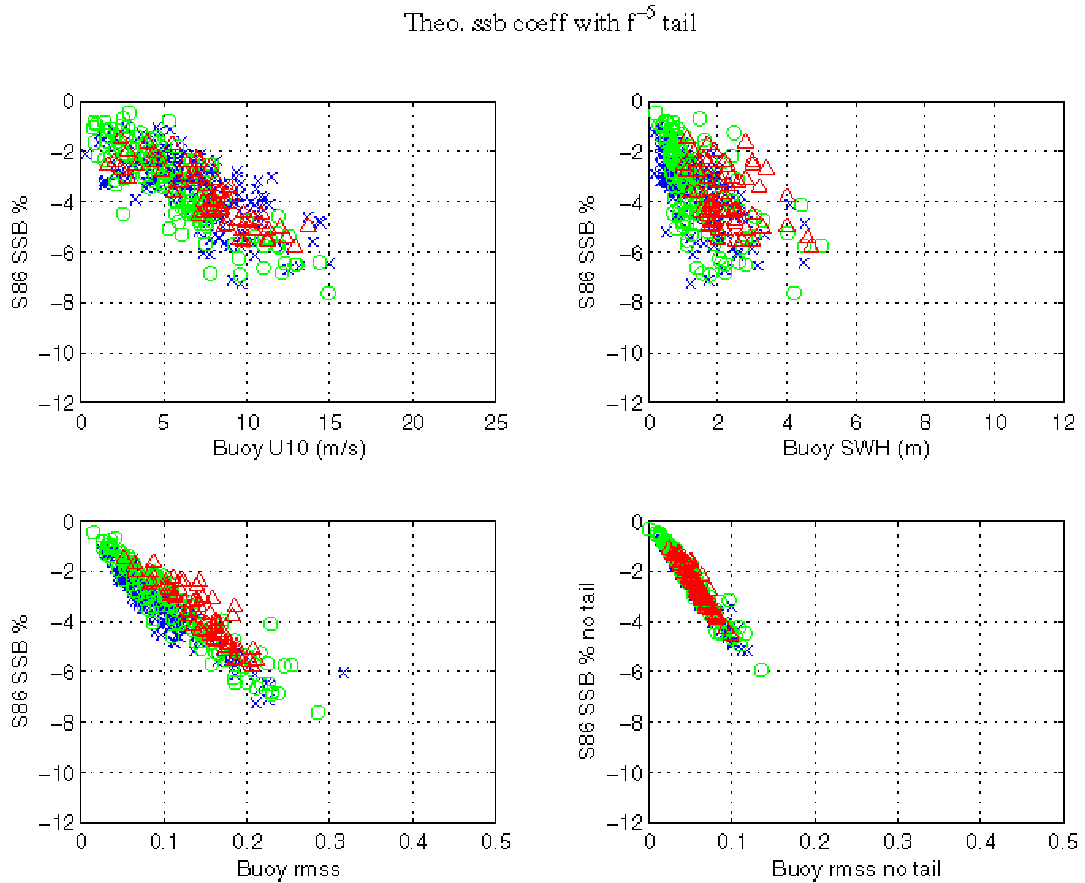


Figure 6.4: Theoretical SSB coefficient after Srokosz (1986) for NDBC directional spectra against (a) buoy wind speed, (b) buoy SWH (c) buoy rms slope in the case of an f^{-5} tail extension, and (d) in the “no-tail” case against rms slope. Key to symbols: ‘x’: Gulf of Mexico (42002), ‘o’: Virginia Beach (44014), ‘Δ’: Hawaii (51026).

6.6 Specifications of the requirements for the new altimeter

The present nominal accuracy of the wind speed and wave height data, as derived from a satellite altimeter, is close to:

wind speed 2 m/s

wave height 0.5 m or 5% of the figure, whichever the larger.

Close inspection and comparison with collocated buoy data indicate that the present performances are somehow better than the above figures. Hence improvement is well within the possibility of a new generation of altimeters.

Such improvement is badly needed in connection with the practical applications of the data. Meteorological and wave numerical models have undergone substantial improvements in the last decade, and the errors expected, and verified, in the open oceans are often of the same order of magnitude of the accuracy of the altimeter derived wind and wave data. One of the most limiting factors in the accuracy of the present forecasts is the accuracy with which we manage to define the situation (analysis) at a certain time. Satellite data represent the most relevant source of data in the open oceans, and their accuracy is therefore critical for an improvement of the accuracy of the meteo- and oceanographic forecasts.

For wind speed a nominal accuracy of 1.5 m/s, with expectation for a somehow better performance, is well within the range of the possible improvement. However, the present accuracy is not evenly distributed in the range of the possible values. The worst performance is achieved for the low and high values of wind speed. But low values characterise extensive areas of the planet. Also, the interest of having more correct wind speeds during the most severe storms is obvious.

While U10, the wind speed at ten metre height, is the official reference quantity in the meteorological world, the key quantity for atmosphere and ocean interactions is the surface stress. Somehow, this is more related to the altimeter response from the sea surface than U10. Hence, in the long term we should consider to derive, and to make use of, this quantity, leaving U10 to eventually more specific uses, e.g. in engineering.

About wave height, extensive comparison between buoy, model and satellite data shows that a 0.25 metre accuracy or better is a realistic assumption for the new altimeters. The performance should be improved also in the high value range, where a 3-4% should be achievable.

The main problem, where improvement is badly needed, is in the coastal zone. Large, if not the largest, economical and social interests are concentrated within a narrow coastal band of the order of a few kilometres. This contrasts with the present capability of the altimeter, when flying offshore, of producing useful data only after a few seconds, hence 20-30 km. Also when flying inshore we find practical limitations, because of the spatial resolution of the data. Both the single measure (presently once every 0.1 second, with a relatively large footprint at the surface) and the averaging technique (once every ten measurements) imply that no data are available close to the coastline. A smaller impact area is highly desirable, together with better consideration of the variability of the signal, reducing the part associated to the instrument itself, and leaving available the one associated to the physics of the surface processes.

It is crucial to point out that substantial improvements in the optimal performance of an altimeter depend not only on the better performance of the instrument itself, but also on the interpretation of the signal, taking into account the physics of the processes. New calibrations are probably an essential step.

In summary, the specifications and recommendations for a new altimeter are shown in details in table A (appendix).

7. Ice Sheet Mass Balance

The mass balance is the net change in mass of ice of a region of the ice sheet. The determination of the growth or shrinkage of the great ice sheets is one of the most important scientific questions of Earth's polar regions and has renewed urgency because of the probable role of grounded ice in sea level change. Effectively, an average negative mass balance over Antarctica could result in a net increase of global sea level.

Recently, the new technologies provided a significant increase in the ability to observe and model ice sheet properties and processes. Useful satellite radar-altimetry data already exist from a series of satellites, dating back to 1978, and data will continue to be acquired for several years. Unfortunately, there are many sources of error in deriving changes in the ice-surface elevation from radar altimeter data, and useful data cannot be presently acquired over slopes larger than about a degree. As we will see more in detail in the following, the estimate of mass balance can be addressed through an integrated approach or a component approach; however, also studies of past changes resulted to be quite instructive.

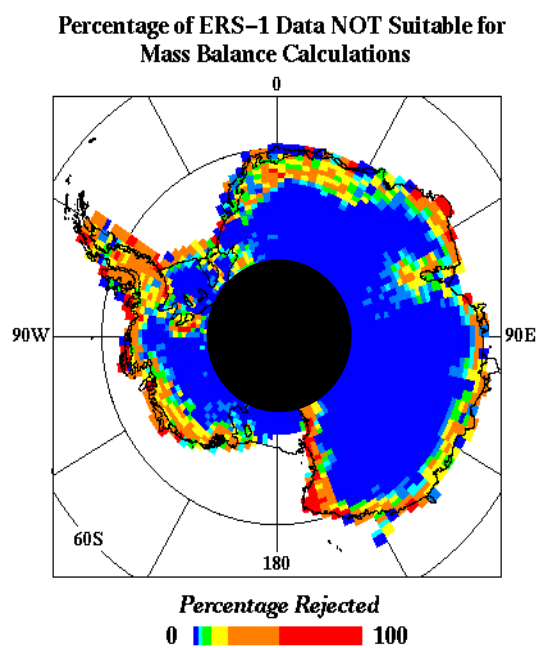


Figure 7.1

The **integrated approach** consists in the measure of changes in ice-surface elevation using satellite altimetry, converting these to estimates of changes in volume by allowing for vertical adjustment of the bed, and finally obtaining an estimate of mass change by applying a correction for changes in near-surface-firn density profiles. Rapidly improving knowledge of satellite orbits has increased the accuracy of this approach (Wingham et al., 1998; Remy et al, 2002; Shepherd et al., 2001).

Crucial for new satellite altimeter mission of ice-sheet studies are surface-elevation changes, optimally measured by laser and/or radar altimeters. The scientific goal should be to determine inter-annual and long-term changes in ice volume, polar

precipitation, and ice melting that may be associated with climate change. New satellite altimeter mission should thus reach higher latitudes (90°) than past satellites (see fig.7.1), have greater elevation accuracy, and an unambiguous determination of the location of the footprint on the surface.

New satellite altimeter mission, with a 5-year lifetime, should be planned as the first in a series of satellites to acquire a time series of ice-sheet elevation change for 15-years, the time needed to accommodate to inter-annual variability in the surface balance and changes in climate in polar regions occurring on decadal-time scales. Continuity of measurements is especially important because of vigorous, well-known oscillatory climatological phenomena such as the North Atlantic Oscillation and El Niño Southern Oscillation, which have a significant impact on Antarctic accumulation rates.

The surface of the ice sheet can rise and fall simply because of snowfall events and density changes in its upper layers (Remy et al., 2002). In particular, fresh, low-density snow causes a rapid increase in surface elevation, followed by a slow decrease as the snow ages and increases in density. The new satellite altimeter mission could depend heavily on time-life measurements that extend over only a few years, so that data interpretation should take into account the short-term, near-surface changes. Synergy with gravity satellite is particularly important in this regard, because the gravity signal response is independent of the density distribution. Inter-annual and long-term elevation changes should be derived with an accuracy of less than 50 mm/yr.

Traditionally, the **component (or flux) approach** to mass balance estimation has been applied to particular areas of interest bounded by ice-flow lines. The measurement area can be quite large: for instance, an entire snow catchment area bounded by an ice divide at its upstream end and the grounding line at its downstream end. The method consists of algebraically summing the mass fluxes across the upstream and downstream boundaries and the upper surface of the measurement area (by snow accumulation). The main input component of ice sheet mass balance is the net accumulation of snow at the surface. Because of large gaps in the observation coverage, any estimate of the current mass input has a large error (Frezzotti et al., 2000). Major gaps in our knowledge of processes that determine the magnitude of the temporal and spatial variability prevent us from making best use of advances in technology and model capability to produce a reliable estimate of current mass input, and prediction of its future trend. New field observations show that the interaction of surface wind and subtle variations of surface slope in the wind direction have a considerable impact on the spatial distribution of snow at short and long spatial scales (Frezzotti et al., 2002a; 2002b). Information about snow surface processes is essential not only for the input term of the mass balance but also for interpreting the surface elevation change signal from the altimeters and for improving the climate and meteorological models. Consequently, inter-seasonal and inter-annual elevation changes should be monitored with an accuracy of less than 50 mm/yr.

In the last 5 years, our picture of a slowly changing Antarctic ice sheet has radically altered. It is now realised that ice shelf basal melting may account for up to one third of the loss from the grounded ice (Rignot 1998; Frezzotti et al. 2000, see also fig. 7.2); extensive, rapid thinning is occurring in one part of the West Antarctic ice sheet interior

(Shepherd et al., 2001; Joughin et al. 2001); and the collapse of the Antarctic Peninsula ice shelves is accelerating the grounded ice discharge (Rott et al., 2002).

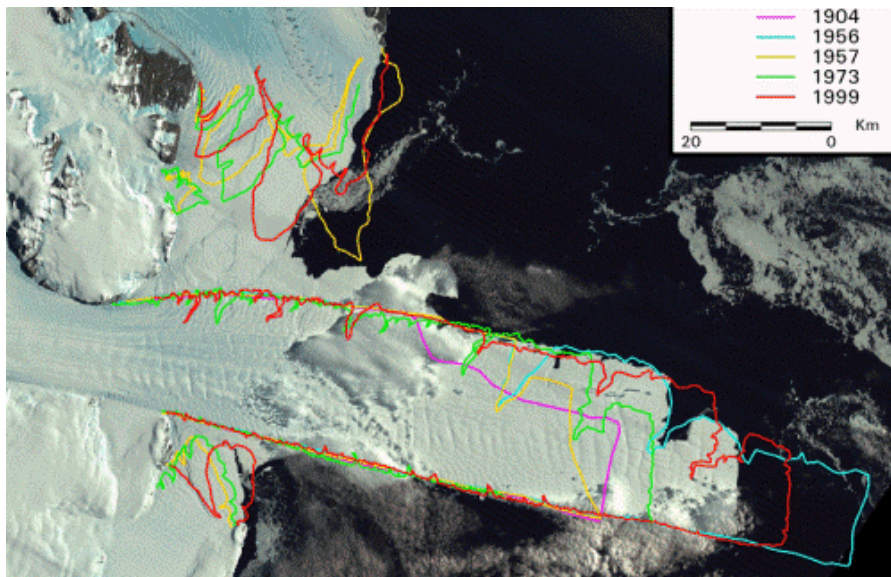


Figure 7.2 Recent ice discharge researches have discovered unexpected higher basal melting (1 or 2 order of magnitude) close to the grounding line of David Glacier and PIG.

The most diagnostic parameter to describe the flow of grounded ice is basal friction. Alteration in the distribution of basal friction is the cause of the major ongoing changes discovered in West Antarctica. To provide a first look at basal friction, measurements of surface slope and estimates of ice thickness are used. New satellite altimeter should generate surface slope data leading to the mapping of basal friction at a spatial scale useful for discussing its magnitude and variation. Digital terrain elevation should then be derived with an accuracy of less than 50 mm/yr.

Oceanic circulation beneath, and melt/freeze interaction with ice shelves has a strong impact on the production of Antarctic Bottom Water (AABW), which serves to ventilate and cool much of the world's deep oceans. A change in the rate of production of AABW as a result of change in sea-ice production or ice-shelf configuration could have a serious impact on patterns of global thermohaline circulation, with attendant consequences for global climate. Unfortunately, the technology for the direct measurement of basal melt/accretion beneath ice shelves does not exist. However, there is the possibility of using a suite of new satellite altimetry to gather detailed measurements of ice thickness near the grounding zones with sufficient accuracy to allow adequate continuity calculations and thereby to infer basal mass balance changing with time in response to changes in ocean conditions. Inter-annual and long-term elevation changes should be measured with an accuracy of less than 50 mm/yr.

Resultant development of Digital Elevation Models (DEMs) could lead to improved maps of balance fluxes/velocities and surface accumulation for investigating the state of mass balance of the Antarctic Ice Sheet.

8. References

- Allen J.T. and D.A. Smeed, 1996: Potential vorticity and vertical velocity at the Iceland-Færøes front, *J. of Phys. Ocean.*, 26, 2611-2634.
- Bosman J., Flemming N. C., Holden N. and K. Taylor, 1998. The EuroGOOS Marine technology survey, *EuroGOOS Publication* No. 4, SOC, Southampton. ISBN 0-904175-29-4.
- Buongiorno Nardelli B., Sparnocchia S., Santoleri R., 2001. Small mesoscale features at a meandering upper ocean front in the western Ionian Sea (Mediterranean Sea): vertical motion and potential vorticity analysis, *J. of Phys. Ocean.*, Vol. 31, 8, 2227–2250.
- Buongiorno Nardelli B., R. Santoleri, S. Marullo, D. Iudicone and S. Zoffoli, 1999: Altimetric signal and three dimensional structure of the sea in the channel of Sicily, *J. Geophys. Res.*, 104, C9, 20585-20603.
- Challenor, P. G. & P.D. Cotton, 2001. The joint calibration of altimeter and in situ wave heights. In, *Guide to the Applications of Marine Climatology, Part II*, WMO, Geneva.
- Chelton, D. B. and M. G. Schlax, Global observations of oceanic Rossby waves, *Science*, 272, pp. 234-238, 1996.
- Chelton D.B., Ries J.C., Haines B.J., Fu L.-L., and Callahan, P.S., 2001. Satellite altimetry in *Satellite altimetry and earth sciences*, edited by L.-L-Fu and A. Cazenave, Academic Press, San Diego, 1-122.
- Chelton D.B. and M.G. Schlax, 2001. The resolution capability of sea surface height fields constructed from a tandem Topex/Poseidon and Jason-1 altimeter mission in *Report of the High-Resolution Ocean Topography Science Working Group meeting*, edited by D.B. Chelton, Oregon State University, 125-145.
- Cipollini, P., D. Cromwell, G. D. Quartly and P. G. Challenor, “Remote Sensing of oceanic extra-tropical Rossby waves”, *Satellites, Oceanography and Society*, ed. D. Halpern, ch. 6, pp. 99-123, Elsevier Science Ltd, 2000
- Cipollini, P., D. Cromwell, P. G. Challenor and S. Raffaglio, “Rossby waves detected in global ocean colour data”, *Geophysical Research Letters*, Vol. 28 , No. 2 , pp. 323-326, 2001.
- Davies & Challenor, 1997. Validation of wave period measurements from radar altimeter data. In *Proc. ASCE Waves 1997 Conference*.
- Elfouhaily, T., D.R. Thompson & L.A. Linstrom, 2002. Delay-Doppler analysis of bistatically refelceted signals from the ocean surface: theory and application. Submitted to *IEEE Trans. Geosc. Rem. Sens*.
- Elfouhaily, T., D. Vandemark, J. Gourrion and B. Chapron 1998 Estimation of wind stress using dual-frequency TOPEX data. *J. Geophys. Res.*, **103**, 25101-25108.
- Fischer J., Flemming N. C., 1999. Operational Oceanography: Data Requirements Survey. *EuroGOOS Publication* No. 12, 59 pp., ISBN 0-904175-36-7.
- Fox A., K. Haines and Beverley De Cuevas, Satellite Data Assimilation in the OCCAM Global Ocean Model *Physics and Chemistry of the Earth*, 24, 375-380, 1999.
- Freilich M. H. & P.G. Challenor, “A new approach for determining fully empirical altimeter wind speed model functions”, *J. Geophys. Res.*, vol. 99, pp. 25051-25062, 1994.

- Frezzotti M., Gandolfi S. and Urbini S.. 2002. Snow megadune in Antarctica: sedimentary structure and genesis. *J. Geophys. Res.* in press,
- Frezzotti M., Gandolfi S., La Marca F. and Urbini S. 2002. Snow dunes and glazed surfaces in Antarctica: new field and remote-sensing data. *Annals of Glaciology* 34, in press.
- Frezzotti M., Tabacco I.E. & Zirizzotti A., 2000. Ice discharge of eastern Dome C drainage area, Antarctica, determined from airborne radar survey and satellite image analysis. *J. Glaciol.* 46, 253-264.
- Fu, L.-L., Recent progress in the application of satellite altimetry to observing the mesoscale variability and general circulation of the oceans, *Rev. Geophys. Space Phys.*, 21, 1657--1666, 1983.
- Fukumori, I., J. Benveniste, C. Wunsch and D. Haidvogel, 1993: Assimilation of sea surface topography into an ocean circulation model using a steady-state smoother . *J. Phys. Ocean.*, 23, 1831-1855.
- Ganachaud, A., C. Wunsch, M.-C. Kim, and B. Tapley, 1997: Combination of TOPEX/POSEIDON data with a hydrographic inversion for determination of the oceanic general circulation. *Geophys. J. Int'l.*, 128, 708-722.
- Gaspar, P., Ogor F., Le Traon P.-Y., and Zanife O.-Z., 1994. Estimating the sea state bias of the TOPEX and POSEIDON altimeters from crossover differences, *J. Geophys. Res.*, 99, 24981-24994.
- Gaspar P. & Florens J-P, 1998, Estimation of the sea state bias in radar altimeter measurements of sea level: Results from a new non-parametric method, *J. Geophys Res.*, 103, 15803-15814.
- Gaspar, P. and C. Wunsch, Estimates from altimeter data of barotropic Rossby waves in the northwestern Atlantic Ocean, *J. Phys. Oceanogr.*, 19(12), pp. 1821-1844, 1989.
- Gill, A. E., *Atmosphere-ocean dynamics*, Academic Press, New York, 1982.
- Glazman R.E. & A. Greysukh, "Satellite altimeter measurements of surface wind", *J. Geophys Res.*, vol. 98, pp. 2475-2483, 1993.
- Gommenginger, C.P., M.A. Srokosz, P.G. Challenor & P.D.Cotton. 2002a, Development and validation of altimeter wind speed algorithms using an extended collocated buoy/Topex dataset. *IEEE Trans. Geosc. Rem. Sens.*, in press.
- Gommenginger, C.P., M.A.Srokosz, J.Wolf, & P.A.E.M Janssen. 2002b, A theoretical investigation of altimeter sea state bias. Submitted.
- Gourrion. J., Vandemark, D., Bailey, S. and Chapron, B., 2000, Satellite altimeter models for surface wind speed developed using ocean satellite crossovers. *Report IFREMER-DROOS-2000-02*, 60 pp. Available from <http://topex.wff.nasa.gov/docs/docs.html>.
- Greenslade D.J.M, D.B. Chelton and M.G. Schlax, 1997. The mid-latitude resolution capability of sea level fields constructed from single and multiple satellite altimeter datasets. *J Atmos. Oceanic Technol.*, 14, 849-870.
- Hill, K. L., I. S. Robinson, and P. Cipollini, "Propagation characteristics of extratropical planetary waves observed in the ATSR global sea surface temperature record", *J. Geophys. Res.*, v. 105(C9), pp. 21,927-21.945, 2000.
- Housego-Stokes, R.E., and P. G. Challenor An interesting four year signal in North Atlantic sea surface temperature anomalies , submitted to *Int. Journal of Climatology*, 2002.

- Huntley, M. E., M. Zhou, et al. (1995). Mesoscale distribution of zooplankton in the California Current in late spring, observed by Optical Plankton Recorder. *J. of Mar. Res.* 53: 647-674.
- Iudicone, D., S. Marullo, R. Santoleri, and P. Gerosa, 1998: Sea level variability and surface eddy statistics in the Mediterranean sea from TOPEX/POSEIDON data, *J. Geophys. Res.*, 103, 2995-3012.
- Jacobs, G. A., H. E. Hurlburt, J. C. Kindle, E. J. Metzger, J. L. Mitchell, W. J. Teague, and A. J. Wallcraft, Decade-scale trans-Pacific propagation and warming effects of an El Niño anomaly, *Nature*, 370, pp. 360-363, 1994.
- Joughin I., Gray L., Bindshadler R., Price S., Morse D., Hulbe C., Mattar K., Werner C. 1999. Tributaries of West Antarctic Ice Stream revealed by RADARSAT interferometry. *Science*, 286, 283-286.
- Killworth, P. D., and Blundell, J. R., The effect of bottom topography on the speed of long extratropical planetary waves. *J. Phys. Oceanogr.*, 29, pp. 2689-2710, 1999.
- Killworth, P. D., D. B. Chelton and R. de Szoeke, The speed of observed and theoretical long extra-tropical planetary waves. *J. Phys. Oceanogr.*, 27, pp. 1946-1966, 1997.
- Larnicol, G., N. Ayoub and P.Y. Le Traon, 2002: Major changes in the Mediterranean Sea level variability from seven years of Topex/Poseidon and Ers-1/2 data, to appear in June 2002 in *J. of Mar. Sys.*
- Le Provost, 2001. Tides over ridges, shelves and near the coasts, in *Report of the High-Resolution Ocean Topography Science Working Group meeting*, edited by D.B. Chelton, Oregon State University, 61-66.
- Le Traon P.-Y., and G. Dibarboure, 1999. Mesoscale mapping capabilities of multiple-satellite altimeter missions. *J. Atmos. Oceanic Technol.*, 16, 1208-1223.
- Le Traon, P.Y., P. Gaspar, F. Bouyssel, and H. Makhmaraa, 1995: Using Topex/Poseidon data to enhance ERS-1 data. *J. of Atmospheric and Oceanic Technology*, 2, 161-170.
- Le Traon P. Y. and F. Ogor, 1998, ERS-1/2 orbit improvement using Topex/poseidon : the 2 cm challenge, *J. Geophys. Res.*, 103, 8045-805.
- Le Traon P. Y. and F. Nadal and N. Ducet, 1998. An improved mapping Method of multisatellite altimeter data. *J. Atmos. Oceanic Tech.*, 15, 522-533
- Longhurst, A. R. (1995). Seasonal cycles of pelagic production and consumption. *Progress in Oceanography* 36: 77-167.
- Malanotte-Rizzoli P., B.B. Manca, M. Ribera d'Alcalà, A. Theocharis, A. Bergamasco, D. Bregant, G. Budillon, G. Civitarese, D. Georgopoulos, A. Michelato, E. Sansone, P. Scarazzato and E. Souvermezoglou, 1997: A synthesis of the Ionian Sea hydrography, circulation and water mass pathways during POEM-Phase I, *Prog. Oceanog.*, vol. 39, 153-204.
- Marullo S., E. Napolitano, R. Santoleri, B. Manca, R. Evans, 2002. The variability of Rhodes and Ierapetra gyres studied by remote sensing observations, hydrographic data, and model simulations during liwex (October 1994-April 1995). *J Geoph. Res.*, Submitted.
- McGillicuddy Jr, D. J. and A. R. Robinson (1997). Eddy induced nutrient supply and new production in the Sargasso Sea. *Deep-Sea Res.* I 44(8): 1427-1450.
- McPhaden, M. J., The eleven-year El Niño?, *Nature*, 370, p. 326, 1994.

- Millet, F.W., Arnold, D., Gaspar, P., Warnick, K. & Smith, J., 2002. Electromagnetic bias estimation using in situ and satellite data: a nonparametric approach. Submitted.
- Morrow, R., R. Coleman, J. Church, and D. Chelton, Surface eddy momentum flux and velocity variances in the Southern Ocean from Geosat altimetry, *J. of Phys. Oceanogr.*, 24, 10, 2050-2071, 1994.
- Oschlies, A. and V. Garçon (1998). Eddy-induced enhancement of primary production in a model of the North Atlantic Ocean. *Nature* 394: 266-269.
- Pinardi N. and N. C. Flemming, 1998. The Mediterranean Forecasting System Science Plan, *EuroGOOS Publication* No. 11. SOC, Southampton, 48pp., ISBN 0-904175-35-9.
- Pinardi, N., F. Auclair, C. Cesarini, E. Demirov, S. Fonda-Umani, M. Giani, G. Montanari, P. Oddo, M. Tonani, M. Zavatarelli, 2002. Toward marine environmental predictions in the Mediterranean Sea coastal areas: a monitoring approach. *In: Ocean Forecasting* (N. Pinardi and J. Woods Eds.) Springer & Verlag.
- Pinardi N., I. Allen, E. Demirov, P. De Mey, A. Lascaratos, P-Y. Le Traon, C. Maillard, G. Manzella, and C. Tziavos, 2002. The Mediterranean ocean Forecasting System: first phase of implementation (1998-2001). Submitted to *Annales Geophysicae*, MFSPP special issue.
- Prandle D. and N. C. Flemming, 1998. The science base of EuroGOOS, *EuroGOOS Publication* No. 6, SOC, Southampton. ISBN 0-904175-30-8
- Quarty, G.D. 1998 Determination of oceanic rain rate and rain cell structure from altimeter waveform data. Part I: Theory, *Journal of Atmospheric and Oceanic Technology*, 15, 1362-1379.
- Remy F., Testut L. & Legresy B. 2002. Random fluctuations of snow accumulation over Antarctica and their relation to sea level change. *Climate Dynamics*, in press.
- Rignot, E.J. 1998. Fast recession of a West Antarctic glacier. *Science*, 281(5376), 645-656).
- Rott H., Rack W., Skvarca P. and De Angelis 2002. Northern Larsen Ice Shelf, Antarctica: further retreat after collapse. *Annals of Glaciology* 34, in press
- Shepherd A., Wingham D.J., Mansley J., and Corr H. 2001 Inland thinning of Pine Island Glacier, West Antarctica. *Science*, 291.
- Samelson R.M. and D.C. Chapman, 1995: Evolution of the instability of a mixed-layer front, *J. Geophys. Res.*, 100, C4, 6743-6759.
- Siegel, D. A., The Rossby rototiller, *Nature*, v. 409, pp. 576-577, 2001.
- Srokosz, M. A. 1986. "On the joint distribution of surface elevation and slopes for a nonlinear random sea, with an application to radar altimetry", *J. Geophys. Res.*, 91, 995-1006, 1986.
- Spall M.A., 1995: Frontogenesis, subduction and cross-front exchange at upper ocean fronts, *J. Geophys. Res.*, 100, C3, 2543-2557.
- Stammer, D., Wunsch, C. and Ponte, R. M., De-Aliasing of Global High Frequency Barotropic Motions in Altimeter Observations, *Geophys. Res. Lett.*, 27(8), pp. 1175-1178, 2000.
- Stammer, D., 1997: GEOSAT Data Assimilation with Application to the eastern North Atlantic, *J. Phys. Oceanogr.*, 27, 40-61.
- Sutton, R. T., and Allen M. R., Decadal predictability of North Atlantic sea surface temperature and climate, *Nature*, 188, pp. 563-567, 1997.

- Taylor, P.K. & M. J. Yelland, 2001. The dependence of sea surface roughness on the height and steepness of the waves. *J. Phys. Ocean.*, 31, 572 – 590.
- Uz, B. M., Yoder, J. A. and Osychny, V. Pumping of nutrients to ocean surface waters by the action of propagating planetary waves, *Nature* v. 409, pp. 597–600, 2001.
- Williams, R. G. and M. J. Follows (1998). Eddies make ocean deserts bloom. *Nature* 394: 228-229.
- Wilkin, J., and R. A. Morrow, Eddy kinetic energy and momentum flux in the Southern Ocean: Comparison of a global eddy-resolving model with altimeter, drifter and current-meter data, *J. Geophys. Res.*, 99(C4), 7903-7916, 1994.
- Wingham D.J., Ridout A.J., Scharoo R., Arthern R.J., Shum C.K. 1998. Antarctic elevation change from 1992 to 1996. *Science* 282,456-458.
- Witter D.L., & D.B. Chelton, “A Geosat altimeter wind speed algorithm and a method for altimeter wind speed algorithm development”, *J. Geophys Res.*, vol. 96, pp. 8853-8860, 1991.
- Woolf, D.K., P D. Cotton & P. G. Challenor. 2002. Measurements of the offshore wave climate around the British Isles by satellite altimeter. *Royal Soc. Phil. Trans.* in press.
- Wunsch C., 1989. Sampling characteristics of satellite orbits. *J Atmos. Oceanic Technol.*, 6, 891-907.

Appendix - TableA

Applications/parameters on the oceans	THRESHOLD							OPTIMAL							additional requirements
	Spatial resolution	Along-track sampling	Cross-track sampling	accuracy	temporal sampling	mission duration	distance from coast	spatial resolution	Along-track sampling	Cross-track sampling	accuracy	temporal sampling	mission duration	distance from coast	
Large scale circulation/transport	50km	50km	300 km	ongoing T/P-ERS	20 days			25km	25km	100 km	1 cm	10 days			Avoiding tidal alias
Large scale propagating features (Rossby waves)	50km	50km	150 km	2 cm	15 days			25km	25km	50 km	1 cm	10 days			Avoiding tidal alias
Barotropic signals			500 km	3 cm	3 days					300 km	1 cm	1 day			Avoiding tidal alias
Open ocean mesoscale (eddies/fronts)	20km	20km	40 km	ongoing T/P-ERS	10 days			15km	15km	30 km	1-2 cm	10 days			
Semi-enclosed seas circulation	15km	15km	30 km	ongoing T/P-ERS	10 days			10km	10km	25 km	1-2 cm	10 days			
Coastal currents small-mesoscale	15 km	15 km	15 km	ongoing T/P-ERS	5 days		15 km	10 km	10 km	10 km	1-2 cm	3 days		5 km	
Coastal tide	10 km	10 km	10 km	ongoing T/P-ERS	not crucial		10 km	5 km	5 km	5 km	1-2 cm	not crucial		5 km	proper aliasing of tidal signals
Mean sea level	NA	NA	NA	0.5 mm/y		2 decades (combined)		NA	NA	NA	0.1 mm/y		3 decades (combined)		Lowest possible instrumental drift
Data assimilation in OGCM	ongoing T/P-ERS	ongoing T/P-ERS	ongoing ERS	ongoing T/P-ERS	10 days		10 km	10 km	10 km	10 km	1-2 cm	5 days		5 km	priority in accuracy for orbit determination in real time
Data assimilation for regional/coastal models	10 km	10 km	10 km	1-2 cm	5 days			5 km	5 km	5 km	1-2 cm	3 days		1 km	
Wind speed	7km ~ 1s	7km ~ 1s	50km	1.5 m/s	3 days		15 km	0.5/1 km	0.5/1 km	25km	1 m/s	6 h		1 km	values maintained throughout the measurement range (strong winds included)
Wave height	7km ~ 1s	7km ~ 1s	100km	0.25 m or 3% of Hs	3 days		15 km	1 km	1 km	25km	0.15 m or 2% of Hs	6 h		1 km	
Applications/parameters on Ice between 60° and 90° latitude	THRESHOLD						OPTIMAL						additional requirements		
	Spatial resolution	Spatial sampling	accuracy	temporal sampling	mission duration	vertical repeatability	Spatial resolution	Spatial sampling	accuracy	temporal sampling	mission duration	vertical repeatability			
Ice sheet inland mass balance	500 m	500 m	5 cm	1 year	5 years	10 cm	100 m	100 m	5 cm	2 months	5 years	5 cm			
Ice sheet margin mass balance	500 m	500 m	5 cm	1 year	5 years	10 cm	100 m	100 m	2 cm	2 months	5 years	10 cm			
Ice shelf	1 km	1 km	5 cm	1 year	5 years	10 cm	100 m	100 m	2 cm	1 month	5 years	10 cm			
Ice dynamics	500 m	500 m	5 cm	Once		10 cm	100 m	100 m	2 cm	Once		10 cm			
Snow accumulation process	500 m	500 m	5 cm	3 months	5 years	5 cm	50 m	50 m	1 cm	1 month	5 years	5 cm			